Eur. J. Mineral., 35, 589–611, 2023
https://doi.org/10.5194/ejm-35-589-2023

European Journal of Mineralogy
Open Access

Petrological study of an eclogite-facies metagranite from the Champtoceaux Complex (La Picherais, Armorican Massif, France)

Thomas Gyomlai[1], **Philippe Yamato**[1,2], **and Gaston Godard**[3]

[1]Université de Rennes, CNRS, Géosciences Rennes UMR 6118, 35000 Rennes, France
[2]Institut Universitaire de France, 75000 Paris, France
[3]Université Paris Cité, Institut de Physique du Globe de Paris, 75005 Paris, France

Correspondence: Thomas Gyomlai (thomasgyomlai@aol.com)

Received: 27 March 2023 – Revised: 29 May 2023 – Accepted: 29 June 2023 – Published: 2 August 2023

Abstract. The high-pressure metagranite of La Picherais belongs to the Cellier Unit (part of the lower allochthon of the Champtoceaux Complex; Armorican Massif, western France), where it crops out as an undeformed body embedded within the orthogneisses of the Cellier Unit and is closely associated with numerous mafic eclogite lenses and seldom metahornfels. The petrographic observations of this metagranite reveal the presence of well-developed reaction textures: (1) pseudomorph after plagioclase, (2) garnet and phengite coronae at biotite–plagioclase interfaces, (3) garnet and phengite coronae at biotite–K-feldspar interfaces, and (4) garnet and rutile coronae at ilmenite–plagioclase interfaces, attesting that it underwent high-pressure and low-temperature conditions after the granite intrusion and its cooling. The analysis of the coronae and of a xenolith inclusion found in this granite points to pressure (P) and temperature (T) estimates of $P > 1.7$ GPa and $T = 600$–650 °C for the peak of metamorphism. P–T estimates performed on the mafic eclogite collected in the vicinity of the metagranite give values of 2.0–2.2 GPa and 640–680 °C, in good agreement with previous estimates made in other places within the Cellier Unit. The La Picherais metagranite is a key example of undeformed high-pressure metagranite allowing the study of the reactivity and degree of transformation of quartzofeldspathic rocks during subduction and constitutes a Variscan equivalent of the Alpine Monte Mucrone or Brossasco–Isasca metagranitoids.

1 Introduction

Because they are less accurate for pressure (P)–temperature (T) estimation, eclogite-facies felsic rocks have received less attention than their mafic counterparts. However, felsic rock can transform under high-pressure (HP) or even ultra-high-pressure (UHP) conditions as already illustrated by several key natural examples (e.g. Dora-Maira Massif in Western Alps: Chopin, 1991; Tso Morari Massif in India: Palin et al., 2017; Bidgood et al., 2023; the Western Gneiss Region of Norway: Young and Kylander-Clark, 2015; or the Variscan belt: Gil Ibarguchi, 1995; Godard, 2009; Lotout, 2017). These examples constitute evidence that continental crust can also be affected by high-pressure and low-temperature (HP-LT) metamorphism. The transformation of continental material modifies its density, rheology, and chemistry, which can have a significant impact on subduction dynamics, the exhumation mechanisms of HP terranes, and melt fertility (e.g. Young and Kylander-Clark, 2015; Baïsset et al., 2023). However, while HP quartzofeldspathic rocks (e.g. metagranitoids) constitute the main part of the continental crust, they have been poorly studied because (i) they generally do not develop eclogite-facies assemblages (e.g. Palin et al., 2017; Young and Kylander-Clark, 2015) or (ii) they are poorly preserved because of subsequent hydration and deformation during retrogression (Proyer, 2003). Equilibration during the prograde or retrograde path is mainly controlled by fluid infiltration (e.g. Austrheim, 1987) but also deformation (which provides new fluid pathways and decreases the grain size), both increasing the reactivity of the rock (e.g. Gosso et al., 2010; Hobbs et al., 2010). Nonetheless, some poorly deformed and poorly hydrated (i.e. with no free water) metagranitoids still

show partial equilibration at high pressure and without major retrogression, allowing the study of their reactivity and degree of transformation at HP conditions (e.g. Monte Mucrone and Dora-Maira in the Western Alps and Malpica–Tuy in the Iberian Massif: Schorn, 2022).

This study focuses on the HP metagranite of La Picherais located in the Armorican Massif in western France (Fig. 1), which we presented to the participants in the pre-conference field trip of the 14th International Eclogite Conference in 2022. This metagranite is present as undeformed lenses in an orthogneiss matrix and contains HP minerals (e.g. garnet, phengite, clinozoisite and some kyanite) mainly crystallizing as coronae and symplectites at the grain boundary between biotite and feldspar or in pseudomorphs after plagioclase (Fig. 2). This metagranite of La Picherais has been previously described by Lasnier et al. (1973), but its HP overprint has never been recognized as such. It is particularly interesting because it is undeformed with a perfect preservation of the magmatic texture (Fig. 2a, b) and shows HP textures that are similar to other key examples of HP metagranitoids (e.g. Monte Mucrone; Fig. 2e, f). The aim of this paper is to describe in detail the petrology of this key example of undeformed HP metagranite of the Champtoceaux Complex and to provide an estimate of the P–T conditions it underwent in comparison with the nearby eclogite mafic boudins.

2 Geological setting

The South Armorican Domain (Armorican Massif, NW France) is part of the Ibero-Armorican Arc, which extends further west toward the Iberian Peninsula (Galicia and northern Portugal) and has been interpreted as resulting from a collision between the Laurasia and Gondwana continents during the upper Palaeozoic (e.g. Brun and Burg, 1982; Matte, 1991; Ballèvre et al., 2014). In this context, blueschist-facies and eclogite-facies rocks have been formed, attesting to the presence of a palaeo-subduction zone and highlighting the presence of ancient suture zone(s).

However, there are actually at least two concentric belts of HP metamorphism in the Ibero-Armorican Arc: (a) towards the interior of the arc, a blueschist-facies belt (or Groix Unit) consists of glaucophanite, glaucophane eclogite and serpentinite boudinaged within garnet–chloritoid–phengite micaschists; the main occurrences of this belt in the Armorican Massif are Groix Island and the Bois-de-Céné region; (b) arranged parallel to this belt but outward from the arc, other units consist of eclogites, serpentinite, and eclogite-facies paragneiss and orthogneiss. From west to east, the main occurrences are Cabo Ortegal (Galicia), Audierne Bay, the Champtoceaux Complex and the Essarts Unit (Armorican Massif).

2.1 The Champtoceaux Complex

The Champtoceaux Complex (Fig. 1) is located between the South Armorican shear zone and the Nort-sur-Erdre Fault, which coincides with a late Carboniferous coal belt (Sillon houiller de la Basse-Loire). It lies structurally on top of the Mauves Unit and below the Mauges Unit (Fig. 1). The Mauves Unit is constituted by a thick, a priori monotonous, series of metagraywackes (albitic micaschists) whose protoliths are supposed to be Proterozoic (e.g. Ballèvre et al., 2009). The Mauges Unit (in the upper allochthonous position) is made up of a Proterozoic basement (micaschists, amphibolites and metavolcanics), on which a Palaeozoic sedimentary succession lies unconformably. The latter begins either in the Cambrian (Cléré-sur-Layon) or in the Lower Ordovician (Châteaupanne). After the regional geological works of the 19th and 20th centuries, Jean Cogné reinterpreted in 1966 the Champtoceaux Complex as being a deep-rooted "nappe" (Cogné, 1966), made essentially of high-grade metamorphic rocks, in which a set of overlapping slices were subsequently recognized (e.g. Ballèvre and Marchand, 1991; Ballèvre et al., 1994; Fig. 1). The composite middle allochthonous units include the Folies-Siffait Unit (amphibolites and metaperidotites, of oceanic affinity) and the Drain Unit (peridotites and metagabbros, recognized as oceanic). The Champtoceaux Unit, made up of migmatitic orthogneisses probably derived from Cadomian protoliths, migmatitic metapelites and rare lenses of eclogite, is structurally situated between the two oceanic units. The eclogite-facies rocks were exhumed and cooled before being involved in the formation of the final Champtoceaux nappe pile associated with the development of inverted metamorphic zoning (Pitra et al., 2010). The lower slices (lower allochthonous) are mainly composed of leucocratic orthogneiss ("leptynites") derived from Ordovician granitoids (Saint-Mars-du-Désert orthogneiss: Paquette et al., 1984; Cellier orthogneiss: Ballèvre et al., 2002) and metapelites (micaschists) of unknown age, but which are probably also Palaeozoic.

2.2 The Cellier Unit

The Cellier Unit is the lowest slice of the Champtoceaux Complex and is mainly made up of an orthogneiss whose transition with an undeformed metagranite can be occasionally observed (Lasnier et al., 1973) and which encloses numerous metre-sized fine-grained mafic eclogite lenses and very few occurrences of metahornfels. The mafic eclogites were first described scientifically as "eurites grenatiques" by François Dubuisson (1830). They were studied by Lacroix (1891) and Brière (1920) at the same time as the eclogites from the Essarts Unit. Lacroix noted that, unlike the latter, the eclogites from Champtoceaux were generally very fine grained and formed small lenses from 1 m to a few metres, stretched in strongly deformed gneisses. Petrological,

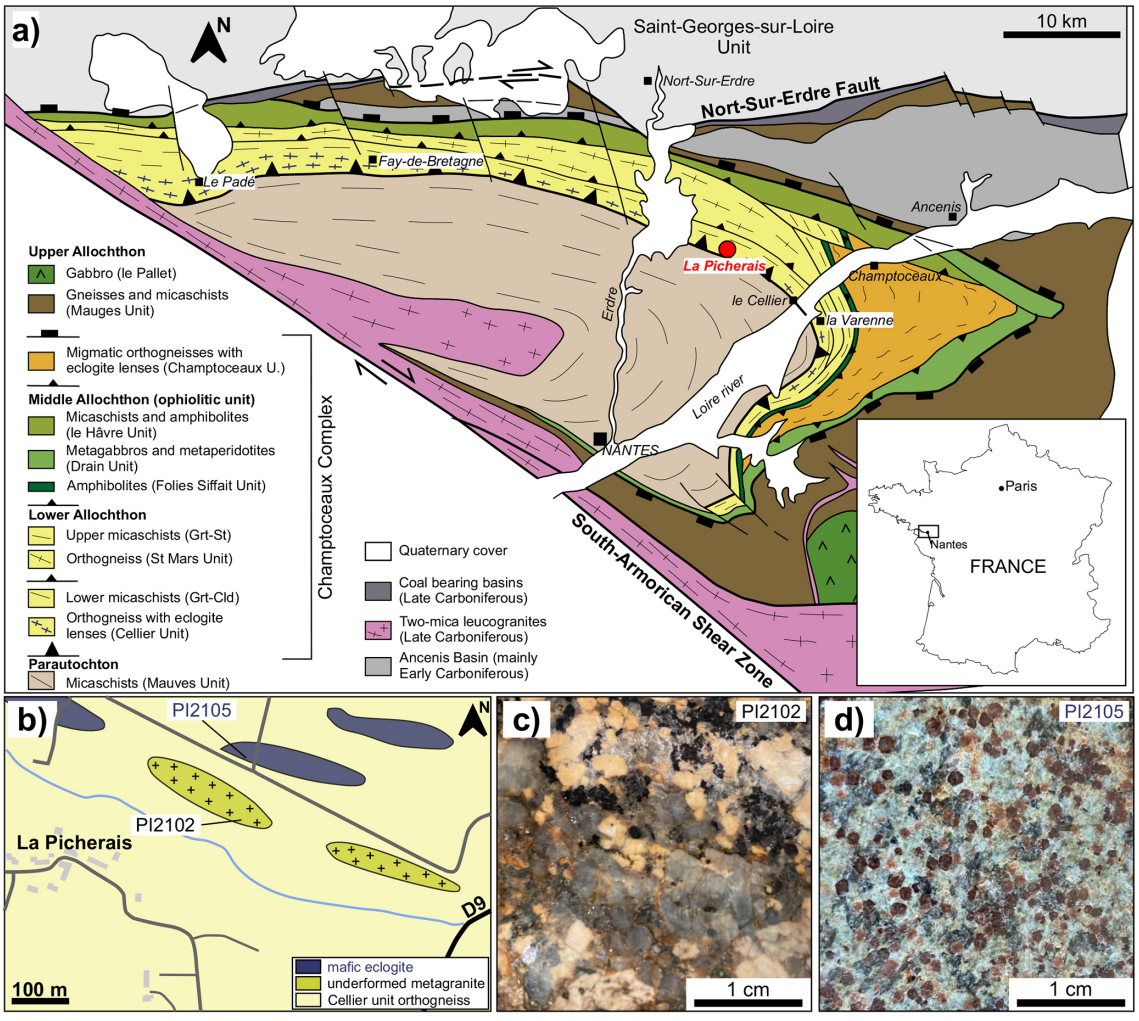

Figure 1. Geological setting of the studied metagranite and eclogite. **(a)** Geological sketch map of the Champtoceaux Complex after Ballèvre et al. (2009). **(b)** Geological sketch map of the studied area modified after Cavet et al. (1978). Photographs of **(c)** metagranite PI2102 and **(d)** mafic eclogite PI2105.

microstructural and geochronological studies were then undertaken on the eclogites (Velde, 1970; Godard et al., 1981; Godard, 1988; Bosse et al., 2000) and the surrounding metagranitoids and orthogneisses (Lasnier et al., 1973; Paquette et al., 1984; Ballèvre et al., 2002). The eclogites contain relics of doleritic textures, and their composition does not show such marked tholeiitic differentiation as in the several-kilometre-sized eclogite bodies of the Essarts Unit, located about 50 km to the southwest (Bernard-Griffiths and Cornichet, 1985; Godard, 1988). It therefore seems that the protolith of these rocks could have been mafic dykes in a thinned granite-rich continental crust (Ballèvre et al., 1994). The metahornfels, well exposed near Campbon particularly at Le Padé quarry (Marchand et al., 1989), are fine-grained massive rocks with biotite, plagioclase and pseudomorphs after cordierite, in which garnet + phengite + rutile + quartz reaction coronae have been observed, similar to those observed in the Cellier metagranite to which they are genetically related (Godard, 2009). An increasing grade of the eclogite-facies P–T conditions from east (La Varenne; 1.5–2.0 GPa, 550 °C) to west (Fay-de-Bretagne; 2.0–2.5 GPa, 650 °C) was documented in the Cellier Unit (Ballèvre and Marchand, 1991). This HP metamorphism was dated at ∼ 360 Ma (Bosse et al., 2000; U–Pb zircon and Sm–Nd garnet dating).

2.3 The La Picherais metagranite

This metagranite was first described by Lasnier et al. (1973) as an undeformed core of some wrongly labelled "charnockitic" granite showing, at its rims, a gradual transition to the strongly deformed orthogneiss in which it is embedded. They attributed this metamorphism to a pre-Cadomian granulite-facies process occurring at high temperature while describing the garnet-forming coronitic reaction between biotite and primary plagioclase, as well as

the transformation of the latter into a pseudomorph of neoplagioclase, white mica and clinozoisite. The discovery and studies of the jadeite-bearing metagranite of Monte Mucrone (Italian Alps; e.g. Compagnoni and Maffeo, 1973) and similar rocks metamorphosed under HP conditions, as well as the vicinity of mafic eclogites, led to the reconsideration of this rock as an HP eclogite-facies metagranite (Girardeau, unpublished data). Dating by the Rb–Sr whole-rock method yielded an errorchron of 570 ± 110 Ma, whereas the U–Pb zircon method provided a lower intercept on concordia at 423 ± 10 Ma (Vidal et al., 1980).

At the outcrop scale (Fig. 1b), this undeformed granite appears as 10 m sized boudins, which change on some decimetres to blastomylonitic orthogneiss by the intermediary of increasingly stretched *augen* gneiss (Lasnier et al., 1973; Cavet et al., 1978). The foliation is concordant with that of the enclosing orthogneiss. The studied samples were taken from boulders of undeformed granite, several metres in size, cropping out at 47°21′1.5″ N, 1°25′41.6″ W. Numerous loose blocks of eclogite are visible in the vicinity, one of which was chosen for the petrological study (PI2105: 47°21′6.1″ N, 1°25′42.8″ W).

3 Methods

3.1 Scanning electron microscope and electron microprobe studies

The studied samples were observed under a scanning electron microscope (SEM) at Paris Sorbonne Université, producing in particular back-scattered-electron (BSE) images and X-ray elemental maps, which were processed using the program XMAPTOOLS 2.2.1 (Lanari et al., 2014).

Electron microprobe (EMP) analyses were carried out at CAMPARIS (SU-IPGP, Paris, France), using CAMECA SX-100 and SX-Five instruments with the data-reducing method of Pouchou and Pichoir (1991). Analytical conditions for spot analysis were 15 kV accelerating voltage and 10 nA specimen current with a beam diameter of 2 µm. Fe_2O_3, $MnTiO_3$, garnet, Cr_2O_3, Ba_2SiO_4, K-feldspar, anorthite, albite and zircon were used as standards. Special conditions of 25 kV accelerating voltage and 10 nA specimen current were used to analyse ZrO_2 in rutile. To estimate the bulk composition of the pseudomorphs after plagioclase, representative areas were analysed by integrating contiguous areas (15 µm × 15 µm) scanned by the electron beam. Representative microprobe data are presented in Table 1.

The mineral compositions obtained were used to balance the hypothetical metamorphic reactions deduced from the observed microstructures, using an algorithm and freeware based on the least-square method (e.g. Godard, 2009; Adjerid et al., 2015). This algorithm provides a vector equation, $\sum n_i\ (\boldsymbol{P}_i) + (\boldsymbol{R}) = (0)$, where vectors $\boldsymbol{P}_i$ are the molar compositions of the i phases involved in the reaction, scalars n_i are the corresponding stoichiometric coefficients, and $\boldsymbol{R}$ is the residual vector resulting from the least-square regression. One n_i is arbitrarily fixed and the others are unknown. Each coordinate of vectors $\boldsymbol{P}_i$ and $\boldsymbol{R}$ corresponds to the content of one independent chemical component. The balance of a reaction is considered satisfactory when (a) the results account for the observed microstructures, with the disappearing and appearing phases as reactants ($n_i < 0$) and products ($n_i > 0$), respectively, and (b) the residuals (i.e. the coordinates of vector $\boldsymbol{R}$) are low, a condition fulfilled when the reaction is almost isochemical.

3.2 Bulk-rock analyses

Two samples, a mafic eclogite PI2105 and a metagranite PI2102, were sent for bulk-rock chemical analyses to ALS geochemistry (Loughrea, Ireland). Sample preparation consisted of fusion with $LiBO_2$ and dissolution in HNO_3. Major elements were analysed by inductively coupled plasma atomic emission spectroscopy (ICP-AES), and trace element concentrations were determined by inductively coupled plasma mass spectrometry (ICPMS).

The bulk compositions of eclogite PI2105 and metagranite PI2102 are presented in Table 2. The same algorithm used to balance the reactions was also applied to calculate the modal proportions of the minerals in each rock, taking into account the molar compositions of the bulk rock ($\boldsymbol{P}_1$) and of the minerals ($\boldsymbol{P}_{i>1}$). The result is considered satisfactory if the residuals are low and the minerals are "produced" from the rock, i.e. if the calculated $n_{i>1}$ values are all positive, whereas the coefficient n_1 for the bulk-rock composition is fixed to -1. The stoichiometric coefficients were converted into volume percentages (Table 2) using the molar volumes given by Abers and Hacker (2016).

3.3 Thermodynamic modelling

The main problem that arises during the thermodynamic modelling of rocks like the metagranite PI2102 is that equilibrium has not been reached at the scale of the rock during metamorphism, since much of the magmatic minerals, still preserved, remained metastable (e.g. K-feldspar, biotite, ilmenite). However, local equilibrium was approached in microdomains, at the scale of the reaction coronae that have grown at the interface of these minerals, so that it is required to model each microdomain instead of the bulk rock. One way to do this is balancing the metamorphic reaction that produced a specific corona by the least-square method. Ideally, if the residuals are low, the overall composition of the products is virtually equal to that of the reactants, representing the atoms that have moved from reactants to products during the reaction and thus can be used as an effective chemical composition to build an isochemical P–T pseudosection (e.g. Godard, 2009; Adjerid et al., 2015). Unfortunately, two complications may arise: (a) one reactant has completely dis-

Table 1. Representative EMP analyses (wt %) of minerals in the mafic eclogite PI2105 and metagranite PI2102. Cor.: coronae.

Mineral group	Garnet								White mica			Ilmenite
Sample	Ilm-Pl cor.	Ilm-Pl cor.	Bt-Pl cor.	Bt-Pl cor.	Bt-Kfs cor.	Xenolith	Mafic	Mafic	Bt-Pl cor.	Xenolith	Bt-Kfs cor.	Ilm-Pl cor.
SiO_2	36.5	37.0	37.1	37.1	37.5	38.3	37.3	38.4	47.7	48.5	48.9	0.0
TiO_2	1.3	0.2	0.0	0.0	0.0	0.0	0.1	0.2	1.1	0.1	1.3	54.5
Al_2O_3	21.2	21.4	21.6	21.8	21.4	22.1	21.6	21.2	30.4	30.9	30.9	0.0
Cr_2O_3	0.0	0.0	0.0	0.0	0.0	0.0	0.0	0.0	0.0	0.0	0.0	0.0
FeO	34.5	27.5	34.0	28.4	37.1	20.6	28.6	21.2	2.6	3.9	2.8	45.6
MnO	1.8	1.2	1.2	0.8	1.5	0.6	0.6	4.7	0.0	0.0	0.0	0.4
MgO	0.7	0.6	3.0	1.5	2.8	3.4	2.6	5.1	2.7	2.1	2.2	0.2
CaO	5.4	11.4	3.3	11.4	0.9	15.2	9.1	8.7	0.1	1.4	0.0	0.0
Na_2O	0.1	0.1	0.0	0.1	0.0	0.0	0.0	0.0	0.2	0.3	0.2	0.0
K_2O	0.0	0.0	0.0	0.0	0.0	0.2	0.0	0.0	10.7	9.4	10.4	0.0
Total	101.4	99.3	100.3	100.9	101.2	100.4	99.9	99.5	95.4	96.5	96.7	100.8
Si	2.93	2.97	2.97	2.94	3.00	2.97	2.96	3.01	3.20	3.21	3.22	0.00
Ti	0.08	0.01	0.00	0.00	0.00	0.00	0.01	0.01	0.06	0.01	0.07	1.02
Al	2.00	2.03	2.04	2.03	2.01	2.02	2.02	1.95	2.40	2.41	2.40	0.00
Fe_{total}	2.31	1.85	2.27	1.88	2.48	1.34	1.90	1.38	0.14	0.22	0.15	0.95
Mn	0.12	0.08	0.08	0.05	0.10	0.04	0.04	0.31	0.00	0.00	0.00	0.01
Mg	0.08	0.08	0.36	0.17	0.33	0.39	0.31	0.60	0.27	0.21	0.22	0.01
Ca	0.46	0.98	0.28	0.97	0.08	1.26	0.77	0.73	0.01	0.10	0.00	0.00
Na	0.01	0.02	0.00	0.01	0.00	0.00	0.00	0.00	0.02	0.04	0.02	0.00
K	0.00	0.00	0.00	0.00	0.00	0.02	0.00	0.00	0.91	0.80	0.87	0.00
$\sum_{cations}$	8.00	8.01	8.01	8.05	8.00	8.03	8.02	8.00	7.02	6.99	6.96	1.98
#(O.OH)	12	12	12	12	12	12	12	12	11	11	11	3

Mineral group	Biotite		Feldspar				Clinozoisite		Pyroxene	Amphibole		
Sample	Xenolith	Granite	Granite	Ilm-Pl cor.	Bt-Pl cor.	Bt-Kfs cor.	Bt-Pl cor.	Mafic	Mafic	Mafic	Mafic	Mafic
SiO_2	38.7	36.9	66.5	62.0	66.9	68.8	40.4	39.5	56.4	42.2	54.2	54.7
TiO_2	0.0	4.7	0.0	0.0	0.0	0.0	0.0	0.1	0.1	0.9	0.1	0.1
Al_2O_3	19.1	16.9	19.6	23.5	21.3	20.4	33.2	33.0	11.3	15.2	6.3	8.3
Cr_2O_3	0.0	0.0	0.0	0.0	0.0	0.0	0.0	0.1	0.0	0.0	0.0	0.1
FeO	12.0	20.7	0.0	0.3	0.3	0.3	0.5	1.2	2.2	20.3	7.1	4.5
MnO	0.0	0.0	0.0	0.0	0.0	0.0	0.0	0.0	0.0	0.3	0.0	0.1
MgO	15.7	7.9	0.0	0.0	0.0	0.0	0.0	0.2	9.3	5.9	17.7	17.8
CaO	0.0	0.0	0.0	5.5	1.0	0.2	23.4	23.9	14.2	8.9	10.4	8.8
Na_2O	0.1	0.1	4.0	9.0	11.1	11.3	0.5	0.1	6.8	4.0	2.4	3.3
K_2O	9.5	9.3	11.4	0.1	0.3	0.6	0.0	0.0	0.0	0.0	0.0	0.2
Total	95.2	96.6	101.4	100.3	100.9	101.6	98.1	98.1	100.3	97.8	98.2	98.0
Si	2.82	2.78	2.98	2.75	2.91	2.97	3.05	3.00	1.99	6.38	7.54	7.52
Ti	0.00	0.27	0.00	0.00	0.00	0.00	0.00	0.01	0.00	0.10	0.01	0.01
Al	1.64	1.50	1.03	1.23	1.09	1.04	2.95	2.96	0.47	2.71	1.03	1.34
Fe_{total}	0.73	1.31	0.00	0.01	0.01	0.01	0.03	0.08	0.06	2.57	0.83	0.52
Mn	0.00	0.00	0.00	0.00	0.00	0.00	0.00	0.00	0.00	0.04	0.00	0.01
Mg	1.71	0.89	0.00	0.00	0.00	0.00	0.00	0.02	0.49	1.33	3.66	3.64
Ca	0.00	0.00	0.00	0.26	0.05	0.01	1.89	1.95	0.53	1.44	1.55	1.30
Na	0.02	0.01	0.35	0.77	0.94	0.95	0.08	0.01	0.46	1.18	0.64	0.89
K	0.89	0.90	0.65	0.00	0.02	0.03	0.00	0.00	0.00	0.00	0.00	0.04
Sum_{cat}	7.81	7.66	5.01	5.02	5.02	5.00	8.01	8.02	4.01	15.75	15.26	15.27
#(O.OH)	11	11	8	8	8	8	12.5	12.5	6	23	23	23

appeared during the reaction – this is the case of the magmatic plagioclase of the metagranite studied; since its composition is unknown, the reaction cannot be accurately balanced; (b) the residuals for some components are significant, indicating that the system was open to these components during the reaction – this is particularly the case for the reaction at the K-feldspar–biotite interface during which some K_2O is released. For these reasons, we opted for the measurements by image analysis of the overall composition of the products. For each reaction, the volumetric proportions of the corona minerals were estimated by image analysis of SEM chemical maps and converted into molar proportions thanks to the molar volumes given by Abers and Hacker (2016). The proportion of the products combined with their average composition obtained at the EMP allowed us to calculate an overall composition of the products, considered as the local effective

Table 2. Bulk composition for metagranite PI2102 and eclogite PI2105 with calculated mineral volume percentages.

Major elements (wt %)	SiO_2	TiO_2	Al_2O_3	Fe_2O_3	MnO	MgO	CaO	Na_2O	K_2O	Cr_2O_3	P_2O_5	LOI
PI2102	70.50	0.64	14.35	4.62	0.06	1.08	1.25	3.02	4.49	0.00	0.17	1.40
PI2105	48.20	1.55	16.35	12.20	0.21	7.92	11.80	3.18	0.07	0.02	0.08	0.26
Trace elements ($\mu g\,g^{-1}$)	Cs	Rb	Sr	Ba	Th	U	Nb	Ta	Ce	Zr	Y	La
PI2102	5.50	156.00	103.5	987.00	15.95	4.23	11.05	0.90	91.5	324	52.7	47.70
PI2105	0.08	3.10	227	11.10	0.38	0.19	1.90	0.10	12.9	107	31.9	4.70
Trace elements ($\mu g\,g^{-1}$)	Ce	Pr	Nd	Sm	Eu	Tb	Dy	Ho	Er	Tm	Yb	Lu
PI2102	91.50	11.35	44.70	9.56	1.36	1.53	9.23	1.91	5.33	0.78	4.86	0.75
PI2105	12.90	2.20	11.80	3.53	1.36	0.84	5.35	1.16	3.33	0.48	2.96	0.47
Mode (vol %)	Quartz	Biotite	Orthose	Albite	Anorthite	Celsian	Ilmenite	Xenotime	Monazite	Zircon		
PI2I02	31.3	15.0	22.6	23.0	6.6	1.0	0.3	0.01	0.3	0.04		
Mode (vol %)	Quartz	Omphacite	Rutile	Clinozoisite	Paragonite	Garnet	Phengite	Barroisite	Apatite	Zircon		
PI2105	1.9	43.8	1.2	6.5	1.9	32.6	0.3	11.5	0.2	0.02		

chemical composition for modelling. A feedback control was then carried out by checking that the composition obtained was also a linear combination of the reactants, either preserved (biotite, K-feldspar, and/or ilmenite) or disappeared (plagioclase of stoichiometry $Ab_x\ An_{1-x}$).

Since such problems do not arise for the eclogite sample PI2105, which is homogeneous and indeed without relict igneous minerals, an effective chemical composition was estimated (SiO_2 50.80, TiO_2 1.29, Al_2O_3 9.75, FeO 8.28, Fe_2O_3 0.22, MnO 0.14, MgO 12.79, CaO 13.31 and Na_2O 3.42 in mol %) from the bulk-rock composition. Garnet crystals display well-defined zoning with distinct cores. Considering a spheric geometry, the relative composition of the core and rim of the garnet is estimated thanks to microprobe transects and subtracted from the bulk composition (considering all Mn is in the garnet) to infer peak equilibrium conditions. The small quantities of P_2O_5 and K_2O and the corresponding small amounts of apatite and muscovite were subtracted from the bulk composition. The quantity of Fe_2O_3 was estimated by expressing the bulk-rock composition as a linear combination of the average compositions of the peak minerals, the Fe^{3+} amount of which was estimated by stoichiometry (clinozoisite: $Fe^{3+} = Fe_{total}$; omphacite: Fe^{3+} giving 4 cations for 6 O; garnet and amphibole: Fe^{3+} negligible).

Thermodynamic modelling was performed using the Perple-X software (version 6.8.4; Connolly, 1990, 2005). In the absence of carbonates and negligible presence of organic matter in the studied sample, CO_2 was neglected and a fixed water activity of 1 was used for the fluid. The thermodynamic dataset of Holland and Powell (2003) was used with the following set of activity models for solid solutions: garnet, epidote (Holland and Powell, 1998), chlorite (Holland et al., 1998), omphacite (Green et al., 2007), feldspars (Holland and Powell, 2003), white mica (Coggon and Holland, 2002), biotite (Powell and Holland, 1999) and amphibole (Diener et al., 2007; only in sample PI2105).

4 Results

Several samples were studied and two samples were analysed in detail in both the metagranite (PI2102) and mafic eclogite (PI2105) found near La Picherais (Fig. 1b, c, d). The following abbreviations are hereafter used to describe mineral chemistry: $X_{Mg} = Mg / (Mg + Fe_{total})$ and $X_{Na} = Na / (Na + Ca + K)$. Amphibole nomenclature is after Hawthorne et al. (2012). Mineral abbreviations are after Kretz (1983) except for wm for white mica, Phg for phengite, Qz for quartz, Amp for amphibole, Cel for celadonite, Cls for celsian and Car for carpholite.

4.1 Metagranite

The bulk-rock composition of PI2102 indicates it is a peraluminous ($Al / (Na + K + Ca) > 1$ in mole ratio) granite ($SiO_2 = 70.5$ and $Na_2O + K_2O = 7.51$ in wt %) following the classification of Shand (1943) and Le Bas et al. (1986). The protolith was a typical granite composed of quartz, biotite ($X_{Mg} = 0.31$–0.47; $Ti = 0.21$–0.29 atoms per formula unit, apfu), potassic feldspar ($Ab_{5-35}\ An_0\ Kfs_{65-95}$) with albitic perthite lamellae (Fig. 2a) and plagioclase now completely replaced by a microcrystalline albite-rich pseudomorph, in which antiperthitic lamellae are still preserved (Fig. 2b) and show an enrichment in Ba ($Ab_7\ An_0\ Kfs_{88}\ Cls_5$). K-feldspar is now microcline but shows the Carlsbad twinning inherited from the magmatic orthoclase. The average composition of the initial magmatic plagioclase was estimated ($An_{22}\ Ab_{78}$) thanks to the mass-balancing algorithm considering the whole-rock composition as a linear combination of biotite + quartz + K-feldspar + albite + anorthite + ilmenite + monazite + zircon. This combination is used in the Streckeisen diagram (Streckeisen, 1976) to identify the initial rock of PI2102 as a monzogranite (Q (quartz) 37.1, A (alkali feldspar) 28.0 and

P (plagioclase) 34.9, in vol %). Ilmenite, xenotime, monazite and zircon are the main accessory minerals.

The "rapakivi" texture, consisting of a millimetre-thick plagioclase mantling a centimetre-sized ovoid K-feldspar, has been observed once and was also previously described by Lasnier et al. (1973). Several mechanisms can explain this texture (i.e. depressurization or magma mixing); as it has been observed only once and since other K-feldspar crystals are unmantled, it is better explained by magma mixing with the transfer of mantled crystals formed in a hybrid rock to the granite (Vernon, 2016).

Several transformations took place during metamorphism: the replacement of plagioclase and the formation of reaction coronae at the biotite–plagioclase, biotite–K-feldspar and ilmenite–plagioclase interfaces. Quartz is never reacting; however, phengite and garnet replacing biotite may occur at the contact with quartz but always in the continuation of a corona between biotite and feldspar (Fig. 5b).

4.1.1 Pseudomorphs after plagioclase

The former magmatic plagioclase is now completely transformed into a microcrystalline mosaic of plagioclase with varying composition (mainly Ab_{70-100} An_{0-30} Kfs_{0-20}; Fig. 4a), in which minute rodlets of clinozoisite (Fe^{3+} = 0.01–0.05 apfu) and flakes of white mica are found (Figs. 5b, c, 7b, c). Clinozoisite and white mica are less abundant at the rims of the pseudomorphs, determining concentric zones visible under the optical microscope (Fig. 2c), of which it is difficult to say whether they correspond to an inherited zoning of the proto-plagioclase or resulted from steps in the replacement of the latter from its edges. The overall composition of this pseudomorph obtained by EMP scans reveals a decrease in alkali content compared to a real plagioclase ($Si_{2.72-2.81}$ $K_{0.04-0.07}$ $Na_{0.49-0.56}$ $Ca_{0.18-0.28}$ $Al_{1.23-1.31}$ O_8; sum cations: 0.82–0.88), which may be due to incipient kaolinization of albite (potentially explaining the porosity as depicted by black spots in Fig. 5c) and/or to alkali mobility during this metamorphic transformation.

4.1.2 Coronae between biotite and plagioclase

At the contact between biotite and the former plagioclase (Fig. 5), garnet coronae show a clear boundary between an almandine-rich zone (Figs. 4, 5c; Alm_{70-75} Prp_{9-12} Sps_{1-2} Grs_{10-18}) with minute inclusions of rutile, on the biotite side, and a grossular-rich (Figs. 4c, 5c; Alm_{60-68} Prp_{4-9} Sps_{2-3} Grs_{21-34}) quartz-bearing zone, on the plagioclase side, where garnet shows subhedral shapes. A rim of polycrystalline albitic plagioclase (Ab_{90-98} An_{2-7} Kfs_{1-5}) without white mica or clinozoisite but with rare Kfs microcrystals (see Kfs in Fig. 5c) occurs close to the corona, on the plagioclase side, whereas phengitic muscovite (Fig. 4b; Prl_{4-6} Ms_{79-88} Cel_{5-15} Pg_0; X_{Mg} = 0.55–0.65; Si = 3.20–3.24 apfu), with minor rutile inclusions, partly replaced the magmatic biotite I in contact with the garnet corona (Fig. 5c). Phengitic muscovite is partly replaced by late retrograde biotite II (Fig. 5c). The corona is clearly related to the biotite–plagioclase interface, as it ends quite abruptly at the quartz contact, near the biotite–plagioclase–quartz triple points (Fig. 5b, c).

4.1.3 Coronae between biotite and K-feldspar

Garnet coronae are also found between K-feldspar and biotite (Fig. 6). Garnet is poorly zoned (Fig. 4c; Alm_{81-84} Prp_{10-13} Sps_{3-4} Grs_{1-3}) but contains tiny rutile inclusions on the biotite side and quartz inclusions on the K-feldspar side. Polycrystalline albite (Ab_{96} An_1 Kfs_3), quartz and white mica asymmetrically replaced K-feldspar around the coronae. Phengitic muscovite (Fig. 4b; Prl_{1-5} Ms_{78-86} Cel_{10-15} Pg_0; X_{Mg} = 0.64–0.69, Si = 3.19–3.24 apfu) also partly replaced magmatic biotite I in contact with the coronae and is also in turn partly replaced by a late retrograde biotite II (Fig. 6b, c); biotite I, phengitic muscovite and biotite II are in optical continuity. The termination of the coronae is commonly unclear, especially at the K-feldspar–biotite–plagioclase triple points, where the polycrystalline zone with plagioclase + muscovite + quartz that replaced K-feldspar extends laterally along the K-feldspar–plagioclase interface. It is possible that this indistinct termination is related to the local presence of a former plagioclase rim around K-feldspar, inherited from the rapakivi texture, which could have led to complications in the final geometry of the coronae.

4.1.4 Coronae between ilmenite and plagioclase

Similarly to the biotite–plagioclase interface, a garnet corona formed between ilmenite and plagioclase (Fig. 7), with an almandine-rich zone (Figs. 4c, 7b; Alm_{74-78} Prp_3 Sps_4 Grs_{16-19}) on the ilmenite side and a grossular-rich zone (Figs. 4c, 7b; Alm_{58-62} Prp_2 Sps_{2-4} Grs_{33-36}) with quartz inclusions on the plagioclase side. Ilmenite is largely replaced by rutile close to the corona, and a clinozoisite-free rim of polycrystalline plagioclase occurs close to the corona but is slightly richer in anorthite (Ab_{74-89} An_{5-26} Kfs_{0-1}) than similar zones near the biotite–plagioclase interface.

4.1.5 Xenolith

One unique millimetre-sized kyanite-bearing inclusion was observed in the metagranite and investigated (Fig. 8). It mainly consists of garnet (Figs. 4c, 8; Alm_{61-68} Prp_{18-27} Sps_{2-7} Grs_{2-20}) being more calcic when approaching the rim of the xenolith and white mica with a large range of composition (Fig. 4b; Prl_{0-17} Ms_{52-100} Cel_{0-36} Pg_0; X_{Mg} = 0.40–0.80; Si = 3.02–3.51 apfu) and partly replaced by biotite (X_{Mg} = 0.60–0.73; Ti = 0 apfu) and minor chlorite (X_{Mg} = 0.28–0.32). Kyanite occurs as small needles associated with phengite (Fig. 8c) and as potentially inherited millimetric kyanite grains (Fig. 8b). Minor albite and clino-

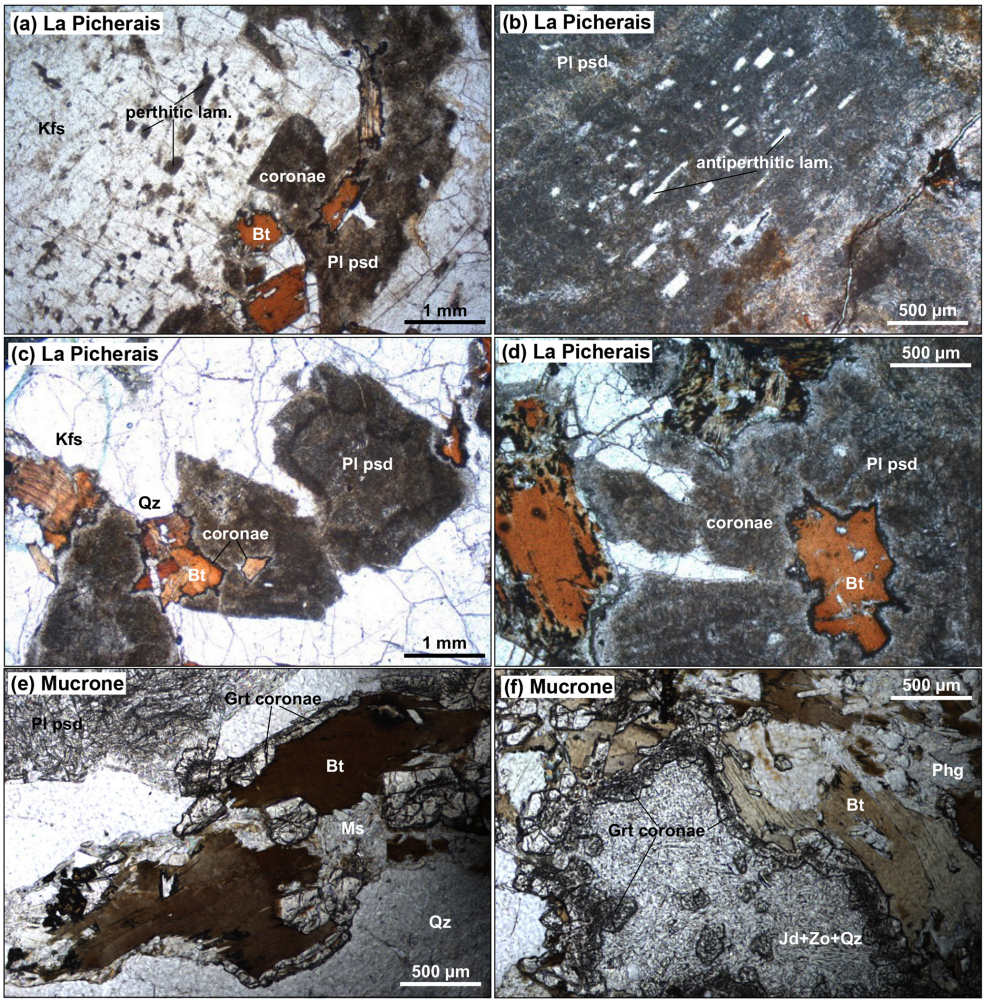

Figure 2. Microphotographs of high-pressure metagranite samples (plane-polarized light). **(a–d)** From La Picherais, in the Armorican Massif: **(a)** K-feldspar with perthitic lamellae (lam.); **(b)** pseudomorph after plagioclase (Pl psd) with antiperthitic lamellae (lam.); **(c)** preserved magmatic texture (Kfs + Pl + Qz + Bt) with zoned pseudomorphs after plagioclase; **(d)** coronae between biotite and plagioclase. **(e, f)** From Monte Mucrone in the Western Alps, with garnet coronae between biotite and quartz **(e)** and between biotite and pseudomorphs after plagioclase **(f)**.

zoisite can be found near the rim of the xenolith and were formed through Ca and Na contamination from the surrounding pseudomorph after plagioclase. One large Ca-rich garnet (Figs. 4c, 8d; Alm_{44} Prp_{13} Sps_1 Grs_{42}) also occurs and is likely inherited. This inclusion likely represents the pseudomorph of an Al-K-rich and Na-poor metapelitic xenolith.

4.2 Mafic eclogite

The bulk-rock composition of PI2105 indicates that its protolith is a basalt or gabbro ($SiO_2 = 48.2$ and $Na_2O + K_2O = 3.25$ in wt %; Le Bas et al., 1986) with a composition close to N-MORB but with a relative enrichment in Th (Th / Yb = 0.13 and Nb / Yb = 0.64), which identifies it as a C-MORB following the classification of Pearce (2008). This composition indicates a continental contamination which is compatible with the previously suggested origin of this eclogite as mafic dykes in a thinned granite-rich continental crust (Ballèvre et al., 1994). The mafic eclogite PI2105 (Fig. 9) is composed of omphacite ($X_{Mg} = 0.81$–0.92; $X_{Na} = 0.42$–0.50), clinozoisite ($Fe^{3+} = 0.05$–0.14 apfu), garnet, amphibole, quartz, paragonite and rutile. Garnet contains inclusions of rutile in both core and rim as well as clinozoisite, omphacite, quartz, and few inclusions of ilmenite and sodic-calcic amphibole in the core (taramite; $X_{Mg} = 0.32$–0.35; $X_{Na} = 0.45$–0.47). Garnet grains are zoned with a decrease of spessartite content from core (Fig. 4c; Alm_{46} Prp_{20} Sps_{11} Grs_{23}) to rim with an intermediate Fe-rich mantle (Fig. 4c; Alm_{63} Prp_{10} Sps_1 Grs_{26}) and an Mg-rich rim (Fig. 4c; Alm_{47} Prp_{30} Sps_0 Grs_{23}). Garnet crystals are in textural equilibrium with omphacite, cli-

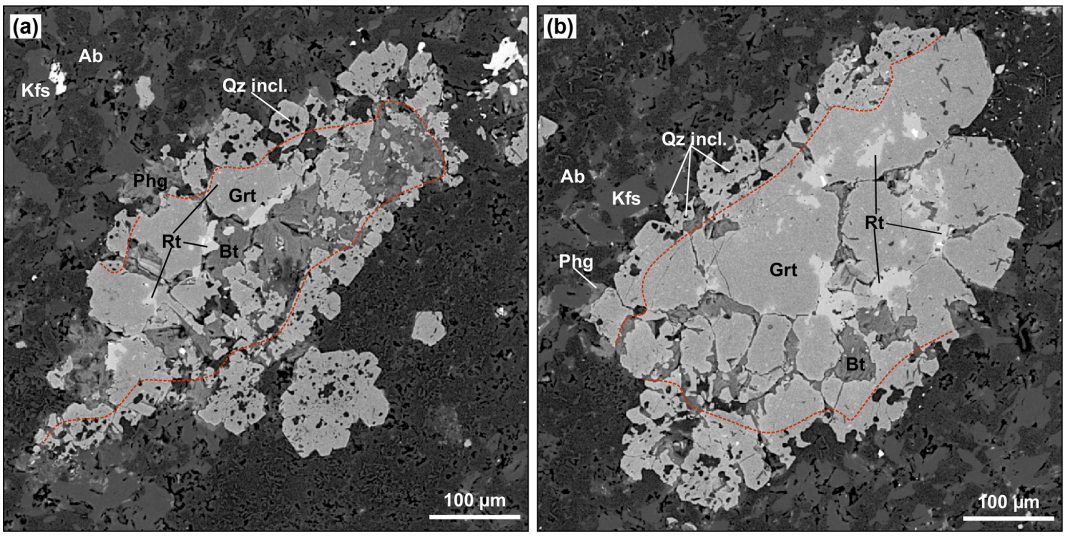

Figure 3. Back-scattered electron images of the metahornfels from Le Padé quarry. Garnet + phengite + rutile + quartz coronae occur between biotite and feldspar and are similar to what is observed in the La Picherais metagranite with the difference of finer biotite grains **(a)** which may be fully replaced **(b)**. The garnet coronae also present a similar internal boundary (dotted red line) between an almandine-rich zone with minute inclusions of rutile, on the biotite side, and a grossular-rich quartz-bearing zone, on the plagioclase side, where garnet shows subhedral shapes.

nozoisite, quartz and rutile, which likely represent the peak paragenesis.

The retrograde assemblage is characterized by plurimillimetric poikiloblastic amphibole porphyroblasts that grew at the expense of the peak paragenesis and enclosed garnet, omphacite and clinozoisite (Fig. 9b, c). The occurrence of amphibole porphyroblasts in the eclogite of the Cellier Unit has been long described since Lacroix (1891), and they were identified as glaucophane in some eclogites (Brière, 1920; Godard et al., 1981) and as brown amphibole, suspected to be barroisite, in others. In the studied eclogite, it is a barroisite ($X_{Mg} = 0.86$–0.90; $X_{Na} = 0.38$–0.42) and may present local magnesio-hornblende composition ($X_{Mg} = 0.78$–0.80; $X_{Na} = 0.28$–0.30) near some clinozoisite or omphacite due to local equilibrium. Balancing the barroisite-forming reaction (see method in Sect. 3.1) yields the following results:

$1.220\ \mathrm{Grt} + 2.564\ \mathrm{Omp} + 0.949\ \mathrm{Qz} + 0.010\ \mathrm{Rt} + 1.493\ \mathrm{H_2O} \rightarrow 1.000\ \mathrm{Amp} + 0.501\ \mathrm{Czo} + 0.242\ \mathrm{Pg} + 1.834$ substitution $\mathrm{Fe_{+1}Mg_{-1}}$ (in molar quantities with almost null residues), which, after transformation into volume amounts, gives a slight increase in volume,

$0.53\ \mathrm{Grt} + 0.60\ \mathrm{Omp} + 0.08\ \mathrm{Qz} + 0.00\ \mathrm{Rt} \rightarrow 1.00\ \mathrm{Amp} + 0.25\ \mathrm{Czo} + 0.13\ \mathrm{Pg}$ (volumes; $\Delta V_{solid}/V_{solid} = +0.119$).

Quartz is apparently the limiting reactant, since it no longer exists as inclusions in the barroisite porphyroblasts (Fig. 9c). Clinozoisite, which predates the formation of barroisite, was partly formed during this reaction and incorporated into the amphibole porphyroblasts in the form of numerous inclusions. Paragonite (Fig. 4b; $\mathrm{Prl_{0-4}\ Ms_{0-12}\ Cel_0\ Pg_{85-100}}$) also occurs in the retrograde assemblage, as well as in a few occurrences with taramite in inclusions in the garnet core. Finally, it should be noted that plagioclase is not present among the products of the reaction, which suggests that the latter, although clearly retrograde, took place under relatively HP conditions.

5 *P–T* evolution

5.1 Eclogite

The *P–T* pseudosection for the mafic eclogite PI2105 (Fig. 10a) was calculated in the NCFMASHTO system with excess water owing to the abundance of hydrated phases (large amount of Czo, Amp and Pg). The *P–T* conditions for the formation of the retrograde barroisite porphyroblasts are constrained around 640 °C and 2.1 GPa by the isopleths X_{Na} (0.39–0.42) and X_{Mg} (0.86–0.90) of this amphibole (Fig. 10a). The peak *P–T* conditions are further constrained around 2.0–2.2 GPa and 640–690 °C, based on the X_{Mg} (0.85–0.89) of omphacite and the Grs fraction (0.23–0.26) of garnet. Under these conditions, the compositions of omphacite ($X_{Na} = 0.46$–0.47) and garnet ($\mathrm{Alm_{41-42}\ Prp_{31-33}\ Sps_{0.8}}$) match satisfactorily those obtained with the electron microprobe except for a slightly higher pyrope fraction (>30). These estimated *P–T* conditions fall within the field Czo + Grt + Omp + Rt + Qz, with predicted modal (vol %) abundances of 43 %–44 % garnet, 2 %–3 % clinozoisite, 50 % omphacite, 1.3 % rutile and 2 %–3 % Qz. The fact that the stability field of the retrograde amphibole is ad-

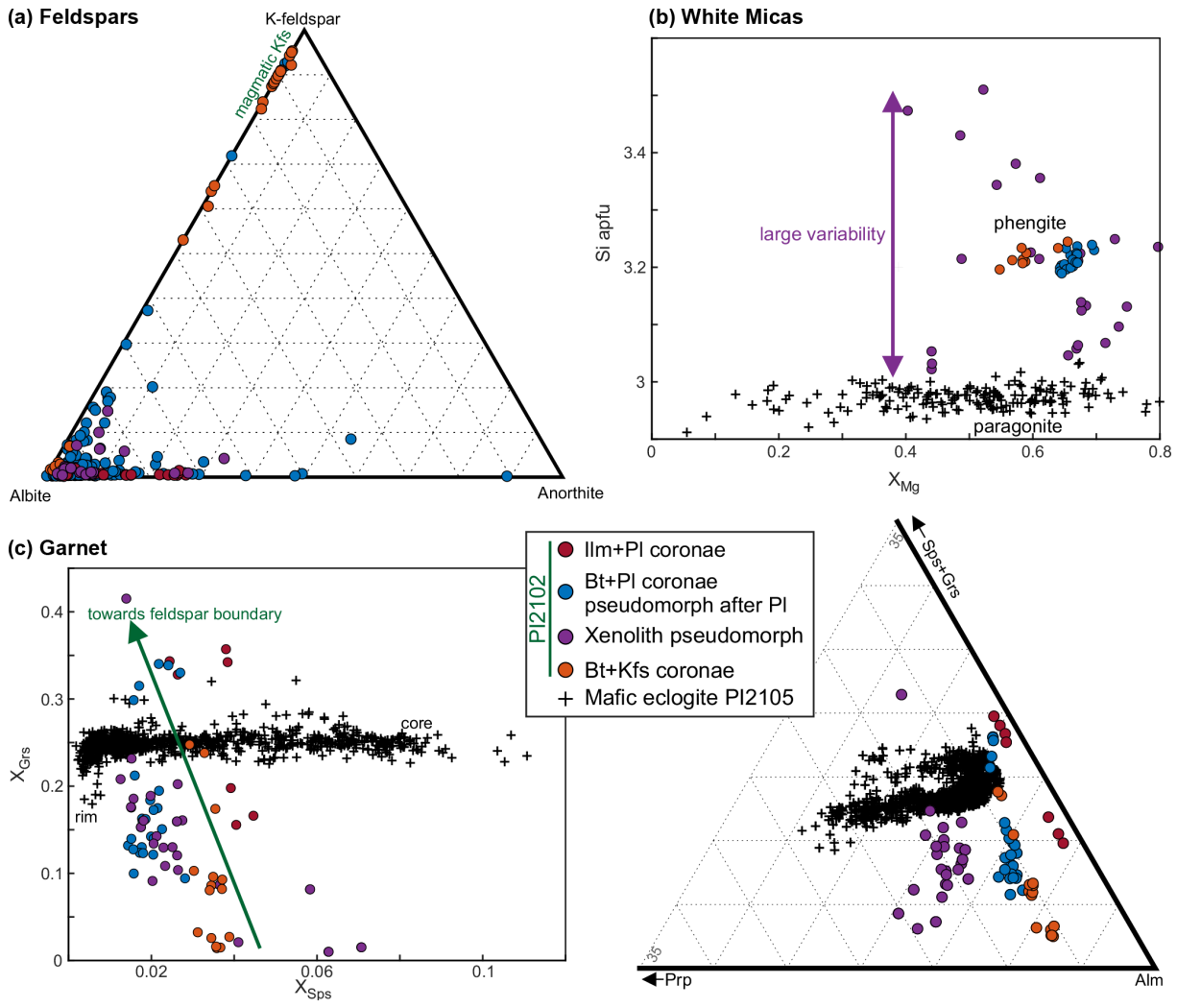

Figure 4. Mineral compositions of the metagranite and eclogite. **(a)** Feldspars in an anorthite–albite–K-feldspar ternary diagram; **(b)** white micas in a Si vs. XMg diagram; **(c)** garnet in a Grs vs. Sps diagram (left) and in a Sps + Grs–Alm–Prp ternary diagram (right).

jacent to the peak P–T field and that the modal abundance of amphibole drastically increases with decreasing temperature suggests an early retrogression of the peak paragenesis (Czo + Grt + Omp + Rt + Qz) with the formation of the large barroisite porphyroblasts at still HP eclogite-facies conditions (∼ 2.0 GPa), outside the plagioclase stability field.

5.2 Metagranite

To clarify the evolution of the pseudomorph after plagioclase, a P–T pseudosection was calculated for the theoretical average composition of the magmatic plagioclase (Fig. 10b; An_{22} Ab_{78}), although the pseudomorph is slightly depleted in alkalis compared to a plagioclase composition, suggesting some alkali mobility during metamorphism (see Sect. 4.1.1). The calculation was performed with an excess of water, given the relatively large amount of clinozoisite and mica in the pseudomorph. The P–T field corresponding to the pseudomorph assemblage (i.e. albite-rich plagioclase + paragonite + clinozoisite + quartz) is found at pressure below the jadeite destabilization curve (green area in Fig. 10b). The peak conditions, estimated from the mafic eclogite, would correspond to the jadeite + paragonite + clinozoisite + quartz field. A lower water content would not change the picture, as it would also produce a peak assemblage with kyanite and/or grossular, associated with jadeite, which are not observed in the pseudomorph.

Estimating the P–T conditions for the formation of the various coronae in the metagranite is arduous because equilibria are only local, with important chemical gradients and a potentially high mobility of some components such as water and alkalis. For example, Schorn (2022) documented large Fe, Mg and Ca gradients in coronae of HP metagranite, resulting in garnet zonations similar to those observed in

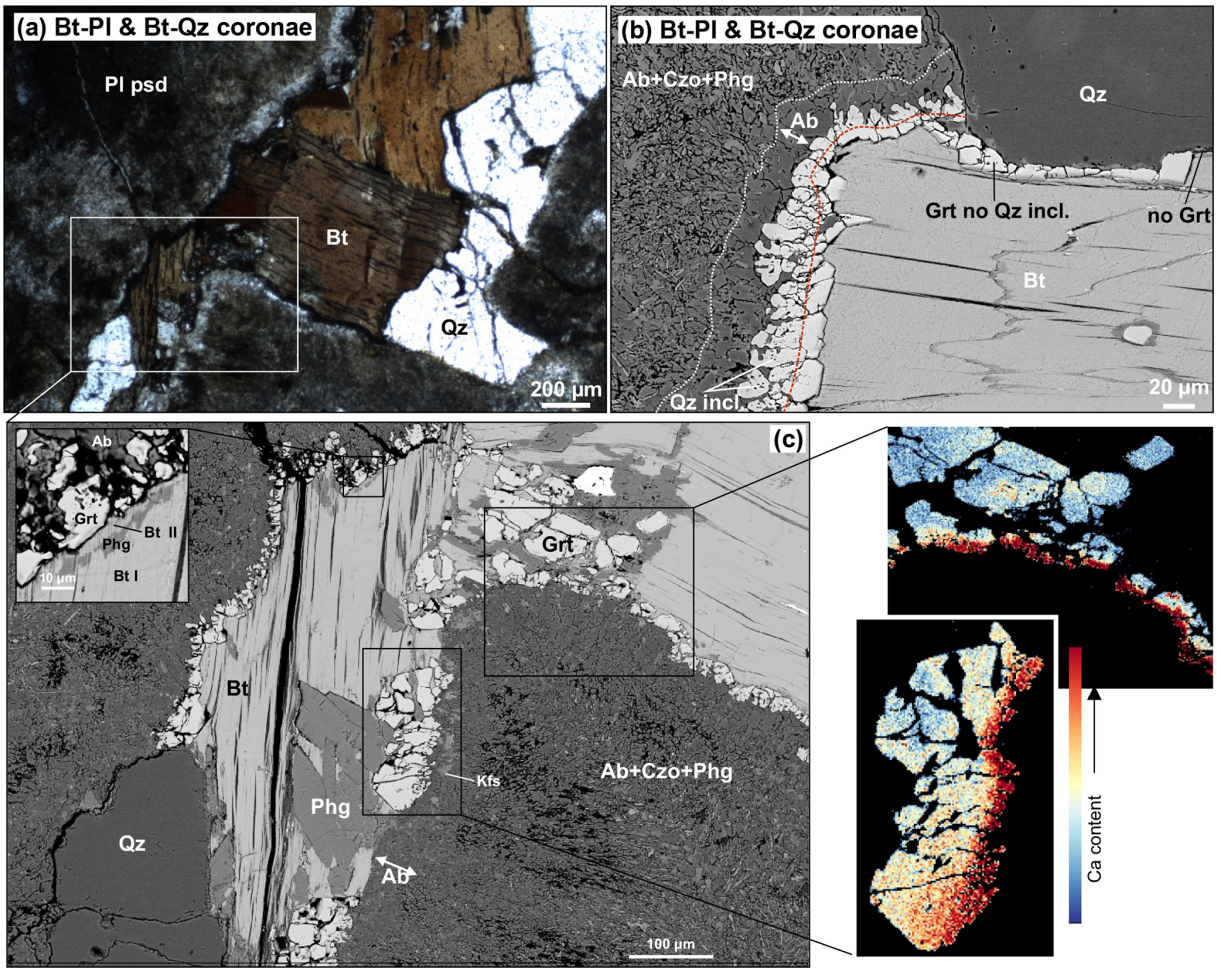

Figure 5. Coronae at the biotite–plagioclase interface. **(a)** Microphotograph (plane-polarized light); **(b, c)** back-scattered electron images and chemical maps of the Ca content in garnet. Magmatic biotite (Bt I) partly replaced by phengite, which is partly replaced by retrograde biotite (Bt II). The dotted red line delineates two garnet zones, one rich in quartz inclusions and the other with only few rutile inclusions. The dotted white line delimits an albite-rich rim around the garnet corona, with few occurrences of K-feldspar.

PI2102. By equilibrating the corona formation reaction at the biotite–K-feldspar interface in a similar rock from the Essarts Unit, Godard (2009) also showed that excess K_2O was produced and likely mobilized by fluids. We therefore focused on local systems that were close to isochemical, except for H_2O. The coronae at the biotite–plagioclase interfaces obey this criterion. On the other hand, balancing the reactions between biotite and K-feldspar (also featuring an asymmetric albitic rim) and between ilmenite and plagioclase yields high residues of Na_2O and K_2O, suggesting their mobility, and this reaction was thus not considered.

Regarding the corona between ilmenite and plagioclase, even if the destabilization of ilmenite to rutile is an indicator of HP metamorphism (e.g. Angiboust and Harlov, 2017), the absence of phengite among the products makes it difficult to estimate whether the corona formed at a higher pressure than the neo-plagioclase rim (An_{18} Ab_{82}), which yields the same P–T stability field as the pseudomorph after plagioclase and may thus be retrograde. The analysis of Zr in the rutile replacing ilmenite provided an average concentration of $68.1 \pm 1.1\,\mu g\,g^{-1}$ (± 2 SE). Following the pressure-dependent thermometer of Kohn (2020), the corresponding temperature is $T(°C) = 39.6 \times P(GPa) + 473.5$, which yields temperature in the range of 533–572 °C between 1.5 and 2.5 GPa. This temperature is significantly lower than the peak conditions estimated from the mafic eclogite and potentially indicates either a retrograde or prograde replacement of ilmenite or a local Zr undersaturation despite the existence of large zircon crystals in the metagranite, meaning that the calculated temperature would therefore represent a minimum crystallization temperature.

A P–T pseudosection was modelled for the coronae at the biotite–plagioclase interface (Fig. 10c). The modal amounts of the products, measured by image analysis of Fig. 5c and converted into molar proportions (0.225 Grt + 0.469 Pl + 0.152 Phg + 0.097 Qz + 0.057 Rt), yielded an effec-

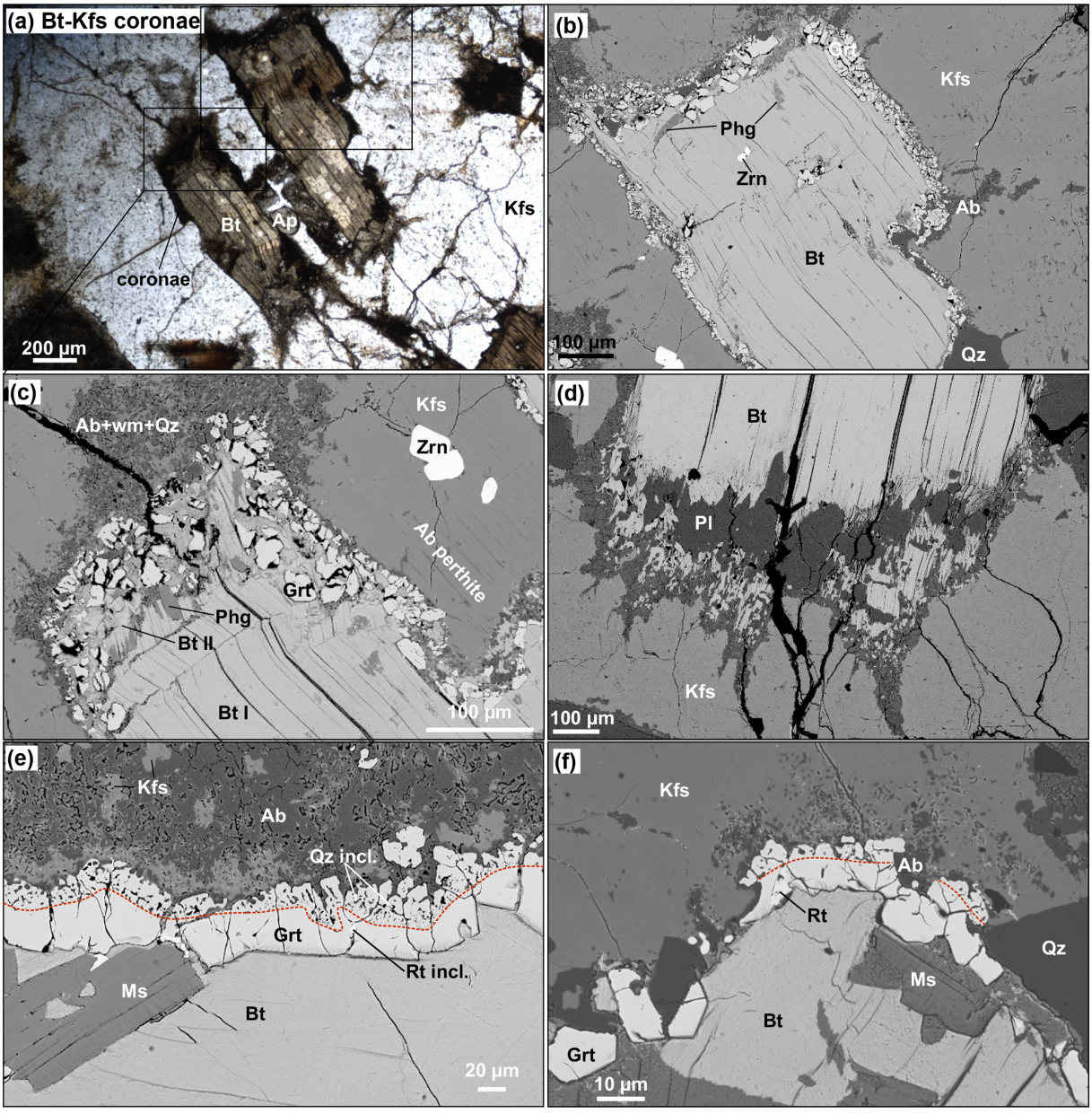

Figure 6. Coronae at the contact between biotite and K-feldspar. **(a)** Microphotograph (plane-polarized light); **(b–f)** back-scattered electron images. **(a)** Weakly transformed K-feldspar with coronae mainly composed of garnet; **(b)** asymmetric albite+garnet+quartz+phengite+rutile coronae; **(c)** K-feldspar and biotite partly replaced by albite + phengite + quartz and garnet + phengite, respectively; **(d)** garnet-free quartz+albite symplectite at the biotite–K-feldspar contact; **(e–f)** K-feldspar asymmetrically and variably replaced by albite and garnet coronae, with dotted red lines delineating two garnet zones, one rich in quartz inclusions and the other with only few rutile inclusions.

tive chemical composition of SiO_2 57.61, TiO_2 1.54, Al_2O_3 14.56, FeO 11.15, Mn 0.28, MgO 2.50, CaO 2.65, Na_2O 4.74 and K_2O 1.62 (mol %). This composition seems to have varied little during the reaction since it produces relatively low residues (SiO_2 −0.003, TiO_2 0.000, Al_2O_3 0.051, FeO −0.004, MgO −0.006, CaO −0.025, Na_2O -0.043 and K_2O −0.047 in molar amounts) when compared to the reactants (1 $An_{22}Ab_{70}$ + 0.421 Bt + 0.159 substitution Fe_{+1} Mg_{-1}) (see the mass-balance algorithm in Sect. 3.1). The mass balancing also indicates that the corona formation produced water (+0.191 H_2O), which is in accordance with Schorn (2022), who suggests that the partial breakdown of biotite produced enough water to hydrate all the pseudomorphs after plagioclase in eclogite-facies metagranites. We therefore considered water in excess. The Si content of the potassic white mica is compatible with the potentially retrograde conditions

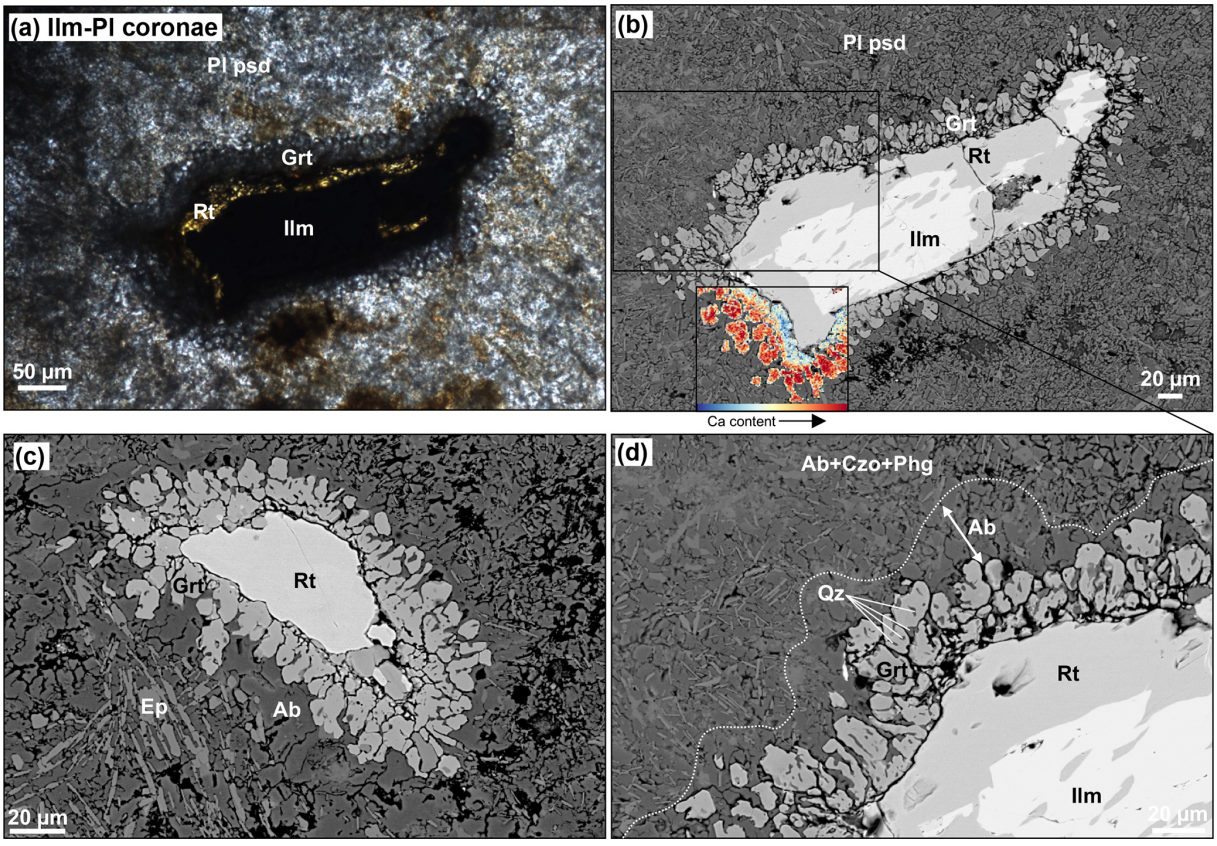

Figure 7. Coronae at the contact between ilmenite and plagioclase. **(a)** Microphotograph (cross-polarized light); **(b–d)** back-scattered electron images, with chemical map of the Ca content in garnet. Concentric rutile and garnet + quartz coronae grew at the contacts between ilmenite and the pseudomorph after plagioclase (see text); ilmenite has been partly preserved **(a, b, d)** or has completely disappeared **(c)**; the dotted white line **(d)** delineates an albite-rich zone around the garnet corona.

estimated for the Ab + Phg + Grt + Rt + Qz field, which corresponds both to the pseudomorph after plagioclase and to the actual mineral composition of the coronae. This Si content is also compatible with the peak conditions estimated for the mafic eclogite, which lie in the jadeite stability field (Omp + Phg + Grt + Rt + Qz; Fig. 10c), whereas this mineral was not observed in the metagranite. Modelled garnet composition (Alm_{70-75} Prp_{11-14} Sps_2 Grs_{10-18}) in the area with Si-rich phengite (Si = 3.20–3.23 apfu) is similar to the composition obtained with the electron microprobe for the dominant almandine-rich garnet. However, the isopleths of garnet were not taken into account as they largely depend on the Ca, Fe and Mg chemical gradients. Lower water content would result in an increase in the stability of kyanite (not observed) and imply a similar trend of the Si content of phengite compatible with both peak and retrograde conditions. Here, we tentatively model the coronae formation by making several assumptions on the local effective chemistry, and the results must be taken with caution. This qualitative result nonetheless corroborates a formation at relatively high pressure (> 1.5 GPa) even if we show that the compositions of garnet (mainly driven by diffusion) and phengite (Si content not acting as a barometer) cannot be used for further constraints.

To check if the metagranite reached the same peak conditions as the mafic eclogite, a pseudosection (Fig. 10d) was modelled for the kyanite-bearing xenolith (Sect. 4.1.5), the composition of which is not controlled by local diffusion, contrary to the coronae. The local composition (SiO_2 46.75, TiO_2 0.002, Al_2O_3 18.16, FeO 13.13, Mn 1.05, MgO 7.88, CaO 0.17 and K_2O 3.99 in molar amounts) was estimated by image analysis in a central zone (Fig. 8c), relatively distant from the inherited garnet of Fig. 8d and from the xenolith border where albite and Ca-rich garnet were likely produced by local chemical contamination from the surrounding pseudomorph after plagioclase. Water was considered in excess because of the large amount of biotite and white mica. The results (Fig. 10d) indicate that an area around 560–610 °C and at $P > 1.7$ GPa in the Grt + Chl + Ky + Bt field fits the local Si content of phengite (3.21–3.25 apfu) and the garnet composition (Grs_1 Sps_6 Alm_{67} Prp_{26}). Predicted modal abundances (vol %) of ∼ 56 % phengite, ∼ 34 % garnet, 6 %–7 % chlorite and 3 %–4 % kyanite agree with observations. The estimated peak conditions of the mafic eclogite are lying

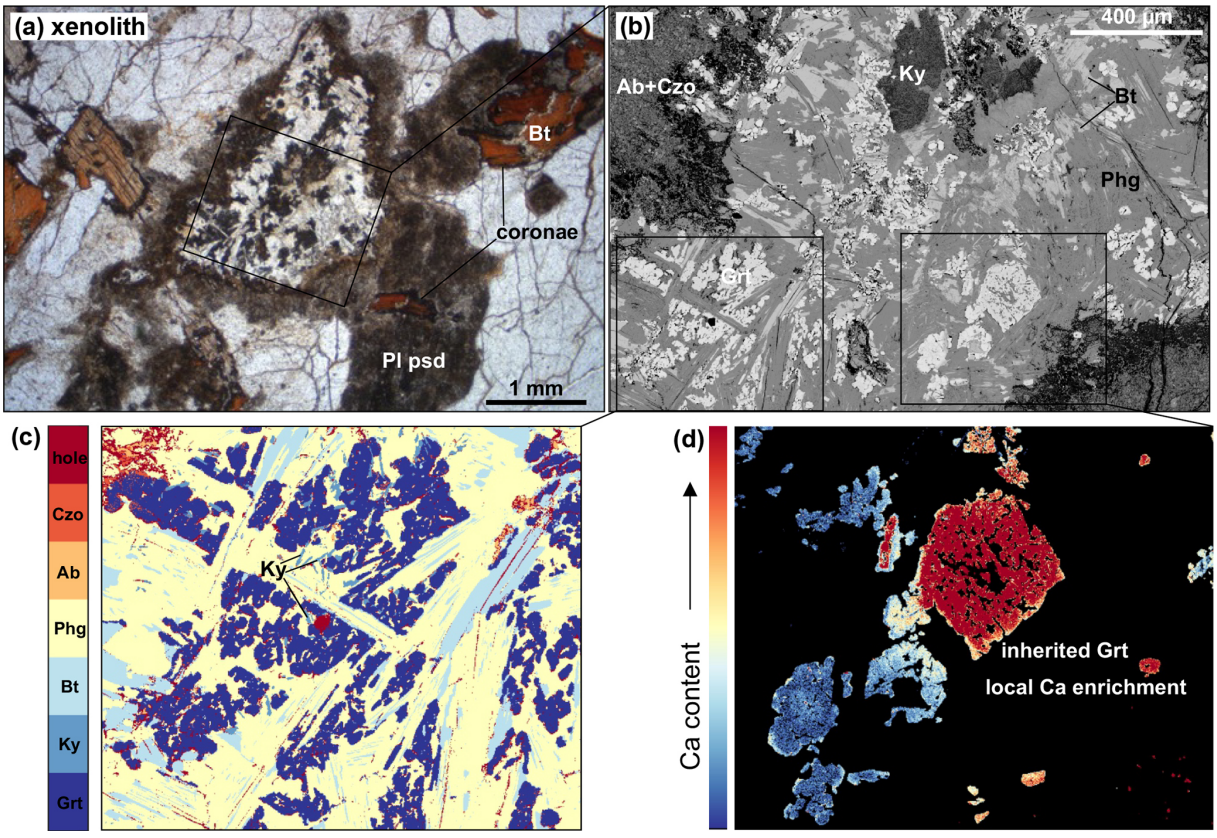

Figure 8. Mica-rich xenolith surrounded by pseudomorphed plagioclase. **(a)** Microphotograph (plane-polarized light); **(b)** back-scattered electron image of the xenolith; **(c)** mineral map of a representative area poorly impacted by Ca or Na contamination; **(d)** chemical map of the Ca content in garnet.

in a field of Mg-rich biotite + phengite + garnet + kyanite, which corresponds to the actual mineral composition of the xenolith with only minor chlorite and phengite partly replaced by biotite. This suggests that the estimated paragenesis of the xenolith corresponds to the late prograde stage of the metagranite.

6 Discussion

6.1 High-pressure metamorphism of the Cellier Unit

As discussed in the previous section, estimating the precise P–T conditions of the formation of the coronae is difficult because the composition of their minerals mainly depends on local diffusion gradients (e.g. Ca, Fe, Mg) and on the amount of H_2O available. We have also shown that the Si content of white mica is poorly constraining (Fig. 10c). Furthermore, corona formation may occur over a large range of P–T conditions, as evidenced by Bruno and Rubbo (2006) for similar metagranitoid of the Monte Mucrone Massif where the garnet coronae would have formed over a range of 0.2 GPa and 100 °C during 2 Ma. Finally, in our case, minerals indicative of clear HP conditions, like jadeite or kyanite, either did not form or were not preserved during retrogression. Nevertheless, the presence of a kyanite-bearing xenolith confirms that the metagranite underwent a pressure higher than 1.7 GPa, which is consistent with the pressure estimated for the nearby mafic eclogite between 1.95 and 2.2 GPa. A slight discrepancy in pressure between the granite and the mafic lenses may be explained by their differences in strength or block aspect ratio (e.g. Moulas et al., 2014; Luisier et al., 2019; Bauville and Yamato, 2021). At such eclogite-facies pressure condition, plagioclase should be unstable with its calcic component transforming into garnet/zoisite + kyanite + quartz ± diopside and its sodic component into jadeite + quartz ± paragonite, depending on the water saturation degree. Neither omphacite/jadeite nor kyanite are observed in the coronae and the pseudomorph after plagioclase of the La Picherais metagranite. The estimated peak P–T conditions are similar to those made in the western part of the Cellier Unit (Fay-de-Bretagne; 2.0–2.5 GPa, 650 °C) and are higher than the estimates made in the east (La Varenne; 1.5–2.0 GPa, 550 °C), which corroborates an increasing grade of the eclogite-facies event from east to west (Ballèvre and Marchand, 1991; Fig. 11).

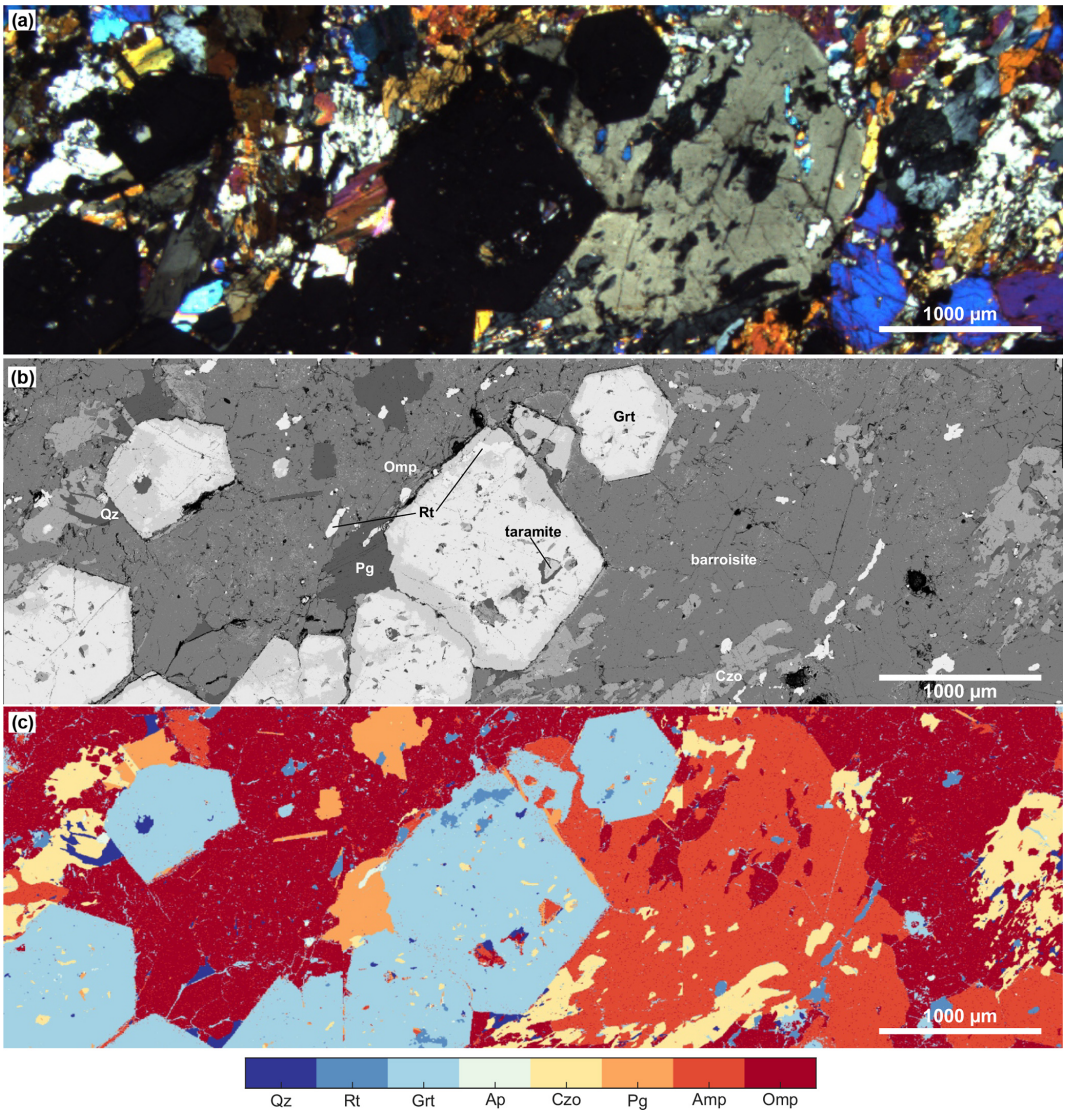

Figure 9. Mafic eclogite PI2105. **(a)** Microphotograph (cross-polarized light), **(b)** back-scattered electron image and **(c)** mineral map of the same representative area.

The Cellier Unit underwent a polycyclic metamorphism (Fig. 11), with a first high-temperature (HT) event consisting of granite intrusion (423 ± 10 Ma; Vidal et al., 1980) and formation of hornfels (e.g. Le Padé; Figs. 1, 3), followed by cooling and then the HP cycle around 360 Ma (Bosse et al., 2000). The first cooling stage is corroborated by the occurrence of antiperthitic exsolution before the HP event with presence of antiperthitic lamellae preserved in the pseudomorph after plagioclase (Fig. 2b). The HP metamorphism affected an already structured thinned continental crust with mafic dyke swarm being eclogitized in the same event as the surrounding felsic rocks, mainly metagranitoids but also metahornfels (Ballèvre et al., 1994; Godard, 2009). The retrograde P–T path, reported very imprecisely in Fig. 11, is little constrained. However, the fact that the omphacite crystals are well preserved, being only replaced by cryptocrystalline symplectites at their very edge, as well as the growth of glaucophane during the retrogression of some eclogites from the Cellier Unit (Godard et al., 1981) suggests a relatively cold exhumation path (Fig. 11), which also seems corroborated by the relative positions of the P–T conditions at the peak and during the barroisite growth in the studied mafic eclogite PI2105 (peak and retro, respectively, in Fig. 10a). Finally, in order to preserve the mineral assemblage that replaced plagioclase in the metagranite, this retrograde P–T path must have followed its stability field ("Pl psd" in Fig. 11) down to fairly low temperatures.

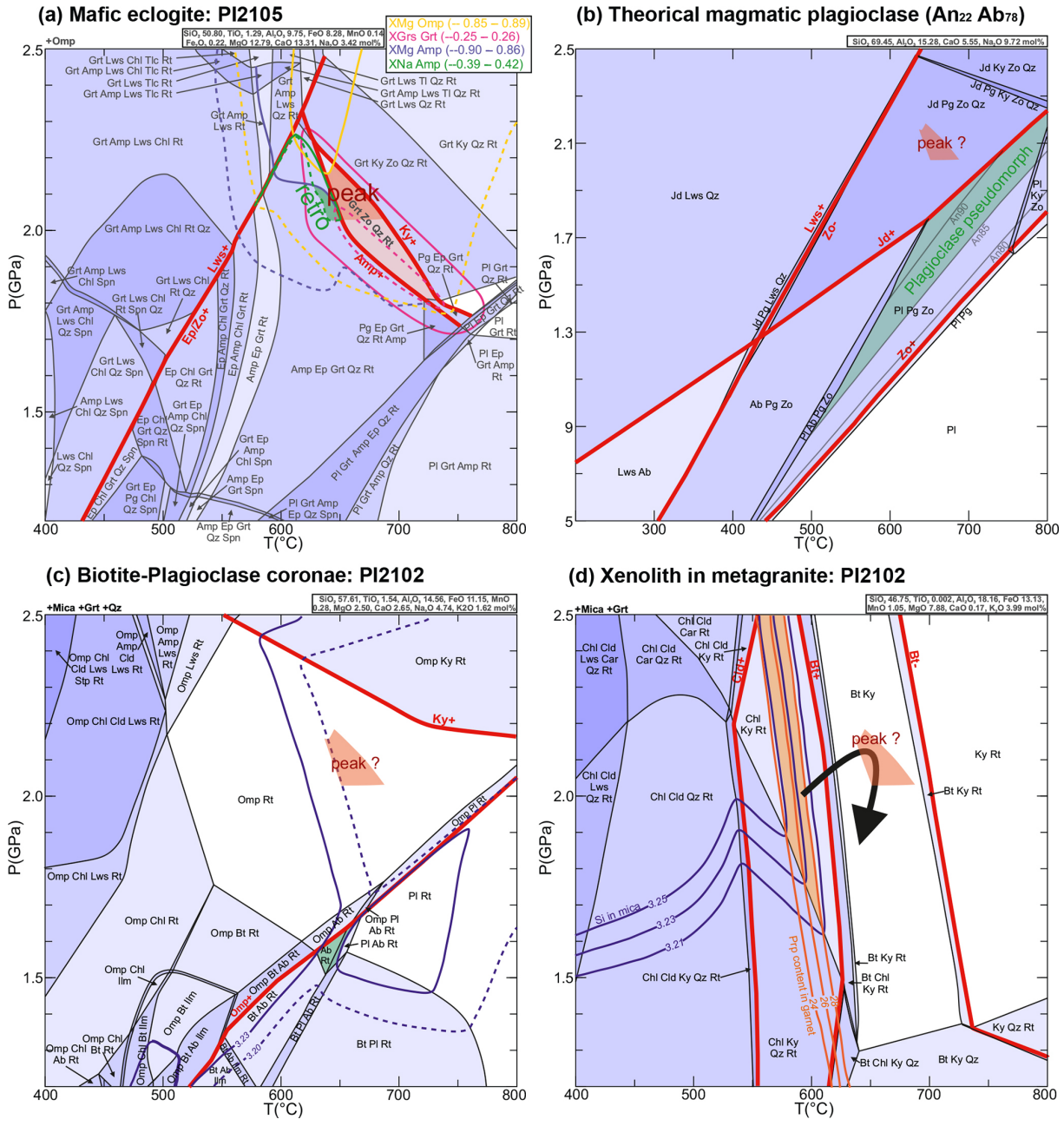

Figure 10. Isochemical P–T pseudosections. **(a)** For the mafic eclogite PI2105; **(b)** for the estimated composition (An_{22} Ab_{78}) of the average magmatic plagioclase, **(c)** a corona between biotite and plagioclase, and **(d)** the xenolith from the metagranite PI2102. Minerals stable throughout the modelled P–T conditions are indicated on the top left of the phase diagrams.

6.2 Comparison with other poorly deformed eclogite-facies metagranitoids

A first comparison can be made with the Malpica–Tuy Unit in the Iberian Massif in NW Spain, which exposes one of the best sections of the Ibero-Armorican Arc (Martínez Catalán et al., 1996; Catalán et al., 2007; Ribeiro et al., 1990). Malpica–Tuy is structurally and petrologically equivalent to the Cellier Unit and is part of the lower allochthon. As in the Armorican Massif, it consists of micaschists and fine-grained orthogneisses derived from Ordovician granites/rhyolites and contains both well-preserved eclogite and poorly deformed metagranitoid boudins. Protolith (∼ 495 Ma: Abati et al., 2010) and HP metamorphism (365–370 Ma: Rodríguez et al., 2003; Abati et al., 2010) ages are similar, and P–T conditions (> 1.6 GPa; 640 °C for the metagranitoids; Gil Ibarguchi, 1995) are also equivalent to the estimates we obtained for the La Picherais metagranite. These two metagran-

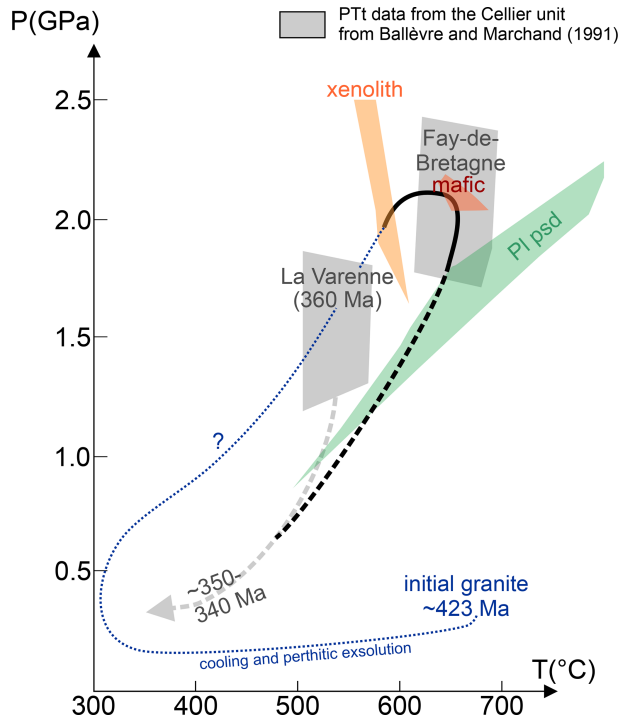

Figure 11. Schematic P–T path of the Cellier Unit. Data from this study and from Ballèvre and Marchand (1991); ages are from Vidal et al. (1980) for the granite formation and from Bosse et al. (2000) for the high-pressure peak and retrograde metamorphism.

ites are similar in all respects according to the description of Gil Ibarguchi (1995): (1) garnet coronae formed between biotite and plagioclase with a rim of albite ± phengite on the plagioclase side and with partial replacement of biotite by white mica, which in turn is partly replaced by secondary biotite; (2) garnet coronae can be found between ilmenite and plagioclase with ilmenite being partly or totally replaced by rutile; and (3) pseudomorphs after plagioclase composed of zoisite, albite and phengite are observed. Unlike our observations, Gil Ibarguchi (1995) documented the presence of jadeite in one locality where barely deformed jadeite-bearing rocks consist of 1 to 10 cm thick porphyritic and aplitic veins that crosscut hornfelsic metasediments enclosed in the orthogneiss. In these veins, jadeite occurs in pseudomorphs after plagioclase but mainly near biotite inclusions, suggesting preferential nucleation of jadeite along grain boundaries. The lack of jadeite in inner parts of pseudomorphs after plagioclase and the irregular development of corona textures indicate fluid restrictions and nucleation barriers during HP metamorphism (Gil Ibarguchi, 1995).

Another comparison should be made with the eclogite-facies gneiss of the Essarts Unit, which is located south of Nantes and of the South Armorican Shear Zone, at barely 50 km from La Picherais. The Essarts Unit is mostly made of continental crust composed of orthogneiss and paragneiss, but it also includes kilometre-scale boudins of mafic eclogites and altered garnet peridotites considered as remnants of a subducted oceanic lithosphere (Godard, 2001, 2009). As in the Cellier Unit, the gneisses underwent two distinct high-grade metamorphic cycles (Godard, 2009), with a first HT and low-pressure event that produced partial melting in the cordierite stability field (migmatitic paragneiss; $T \approx 650\,°C$, $P \approx 0.4$ GPa) accompanied by intrusions of granitoids (now orthogneiss) and followed by a later HP eclogite-facies overprint ($T \approx 700\,°C$, $P > 1.8$ GPa; Godard, 2009). In the ortho- and paragneisses, the HP metamorphism is marked by many pseudomorphic and coronitic reactions, which is more varied than at La Picherais because other HT minerals such as cordierite are involved. Nonetheless, they show similar coronae between biotite and plagioclase (phengite + rutile / garnet + rutile / garnet + quartz / albite), between ilmenite and plagioclase (rutile / garnet / garnet + quartz / albite), and between biotite and K-feldspar (garnet / garnet + quartz / quartz + phengite). The grossular content of garnet also increases near the pseudomorph after plagioclase. A difference with La Picherais is the presence of some kyanite in the pseudomorphs after plagioclase composed of albite–kyanite–zoisite–phengite with kyanite microcrystals delineating polygonal millimetre-sized cells with a honeycomb-like structure that has been interpreted as inherited from the shapes of the HT plagioclase grains. Godard (2009) suggested that the pseudomorphic recrystallization of millimetre-sized albitic single crystals into polycrystalline 10 µm sized albite crystals is likely the result of a phase transition process such as albite to jadeite, which would imply that jadeite crystallized at high pressure before being totally retrogressed into albite (no relic found). Finally, phengite is partly replaced by a late biotite II during the final retrogression. Further south, other Variscan occurrences of gneiss and metagranitoids associated with mafic eclogites and showing similar HP coronae have also been reported in the French Massif Central (see review in Godard, 2009; e.g. Autran and Peterlongo, 1973; Lotout, 2017).

Two other key examples of eclogite-facies metagranitoids containing jadeite belong to the Alpine orogen. These are the Monte Mucrone granitoid in the Sesia Unit (HP event between 500 and 625 °C and 1.3–2.5 GPa: Roda et al., 2012) and the Brossasco–Isasca granitoid in the Dora-Maira Massif (HP event at 730 °C and 4.0–4.3 GPa: Ferrando et al., 2009), both located in the Western Alps. In both cases, the HP overprint is revealed, as in La Picherais metagranite, by pseudomorphs after plagioclase and various coronae at the grain boundaries between magmatic minerals. Similarly to all other examples, the igneous biotite at contact with plagioclase is partly replaced by phengite and rimmed with a garnet corona that contains a few rutile inclusions on the biotite side and is intergrown with quartz on the feldspar side; this garnet also shows a sharp increase in grossular content towards plagioclase (Biino and Compagnoni, 1992; Rubbo et al., 1999; Tropper et al., 1999; Bruno and Rubbo, 2006). The biotite–K-feldspar coronae are similar

to the Essarts coronitic gneisses with a succession of garnet / garnet + quartz / phengite + quartz without albite (contrary to La Picherais metagranite). A major difference of the Monte Mucrone occurrence with the Variscan examples is the presence of a symplectitic rim, in the biotite–plagioclase coronae, composed of phengite + quartz ± jadeite or garnet + jadeite ± phengite ± quartz towards plagioclase. This symplectite is substituted by an albitic rim in the Variscan occurrences. A second difference is that the magmatic plagioclase was pseudomorphed into jadeite-bearing assemblages, typically jadeite + zoisite + K-feldspar + quartz ± kyanite ± phengite at Monte Mucrone (Rubbo et al., 1999; Tropper et al., 1999) and jadeite + zoisite + K-feldspar + quartz + kyanite in the Dora-Maira Massif (Biino and Compagnoni, 1992; Bruno et al., 2001). These major differences could be explained by equilibrium issues, due to kinetic factors (e.g. amount of fluids, residence time), the La Picherais metagranite having been metastable at peak conditions, or by a greater retrogression leading to the full disappearance of jadeite ± kyanite.

6.3 When did the coronae form?

As shown in the previous section, sodic clinopyroxene is generally missing in poorly deformed metagranitoids despite being expected from phase equilibrium calculations. An example is the Tso Morari metagranite which lacks jadeite relic despite reaching the coesite stability field (Bidgood et al., 2023). This is also the case in many HP orthogneisses where sodic clinopyroxene is rarely found (e.g. Young and Kylander-Clark, 2015; Palin et al., 2017). A key example is the Western Gneiss Region (WGR) in western Norway where felsic rocks do not contain clinopyroxene except for isolated cases (e.g. Engvik et al., 2000; Krabbendam et al., 2000; Wain et al., 2001) and rarely contain kyanite despite peak conditions higher than 2.5 GPa (Young et al., 2007; Young and Kylander-Clark, 2015). Therefore, we consider three different scenarios for the La Picherais metagranite, whose HP coronae and pseudomorphs would have formed (1) at peak conditions, with jadeite ± kyanite lately replaced during retrogression; (2) during cooling and exhumation; and (3) during prograde metamorphism, having remained metastable at peak conditions.

To support the first hypothesis, we need clear textural evidence of sodic pyroxene breakdown. However, no pyroxene relic, no Amp + Pl symplectite or pseudomorph after pyroxene was found. The honeycomb-like structure described by Godard (2009) was not observed either. This situation is similar to what Young and Kylander-Clark (2015) described in the WGR (Norway), where sodic pyroxene was not preserved in thousands of square kilometres of HP quartzofeldspathic rocks. In HP orthogneisses, the non-conservation of jadeitic pyroxene could be explained by deformation, hydration and retrogression during exhumation, resulting in the formation of retrograde Pl + Bt salt-and-pepper textures replacing HP parageneses (e.g. Hacker et al., 2010). However, in the case of the undeformed La Picherais metagranite, the HP coronae are perfectly preserved, with only minor retrograde biotite replacing phengite. In addition, the conspicuous presence of albite in the coronae at the biotite–K-feldspar interface suggests the mobility of Na_2O that was not fixed by the crystallization of clinopyroxene. It is therefore difficult to validate the first hypothesis.

The second hypothesis is based on the observation of granulites (White and Powell, 2011; Doukkari et al., 2018; Schorn et al., 2020) and mafic eclogites (Baldwin et al., 2015; Li et al., 2016; Vrabec et al., 2012) in which coronae and pseudomorphs are mainly interpreted as retrograde features formed during slow cooling and exhumation of high-grade metamorphic rocks. The corona textures would have formed because of the high chemical potential between the initial/prograde minerals. At La Picherais, the formation of the coronae and pseudomorphs at the onset of the retrograde path is supported by the composition of some HP minerals, in particular the Si content of phengite in the biotite–plagioclase coronae and the relatively anorthite-rich neo-plagioclase in the pseudomorphs after plagioclase and ilmenite–plagioclase coronae. However, purely retrograde coronae and pseudomorphs imply that no reaction occurred during prograde metamorphism, which could only be explained by fast burial and lack of water. Without evidence for the influx of a retrograde fluid, it appears that most of the water was released during the partial breakdown of biotite (Schorn, 2022), which is typically a prograde process.

The third hypothesis implies a prograde incipient equilibration, predominantly occurring in the stability field of albite, followed by the metastability of the latter in the stability field of jadeite. This hypothesis was suggested for a large number of HP felsic rocks (e.g. Gil Ibarguchi, 1995; Rubbo et al., 1999; Bruno et al., 2001; Young and Kylander-Clark, 2015; Schorn, 2022) and would result from the sluggish kinetics of jadeite crystallization (Young and Kylander-Clark, 2015). A number of kinetic factors such as the availability of fluid, bulk composition and reactivity, and residence time at depth may impede equilibration at high pressures and may prevent the formation of jadeitic clinopyroxene (Heinrich, 1982; Austrheim, 1987; Rubie, 1990; Rumble, 1998; Guiraud et al., 2001; Proyer, 2003; Holyoke and Tullis, 2006; Zhao et al., 2006; Peterman et al., 2009; Spencer et al., 2013; Young and Kylander-Clark, 2015; Schorn, 2022). Nucleation barriers are yet a key parameter for other HP minerals that preferentially crystallized along intragranular cracks or grain boundaries (forming coronae), and nucleation is even more difficult for clinopyroxenes, whose crystallization requires a significant P–T deviation from the producing reaction, or a structurally similar template mineral (e.g. pre-existing clinopyroxene; Wain et al., 2001; Bras et al., 2021), and is facilitated by significant presence of fluid (Rubie, 1998; Schorn, 2022). Schorn (2022) proposed that the

H_2O produced by partial biotite breakdown in metagranitoids is sufficient enough to form HP coronae and pseudomorphs. Nonetheless, he explains that the amount of water needed to reach saturation increases with pressure and its limited availability, in a closed system, may impede jadeite crystallization (Young and Kylander-Clark, 2015; Schorn, 2022).

We suggest that the coronae formed during prograde metamorphism remained metastable in the jadeite stability field because of nucleation barriers and the decreasing availability of water with pressure. The corona minerals, mostly the albite, may have also partly re-equilibrated during retrogression when the water availability increased again.

7 Conclusions

The La Picherais metagranite, localized in the Cellier Unit (Champtoceaux Complex; Armorican Massif), is a key example of undeformed HP metagranite that contains well-developed reaction textures: (1) pseudomorph after magmatic plagioclase; (2) garnet-bearing coronae at biotite–plagioclase interfaces; (3) garnet-bearing coronae at biotite–K-feldspar interfaces, and (4) garnet and rutile coronae at ilmenite–plagioclase interfaces. Despite the difficulty of estimating P–T conditions in quartzofeldspathic rocks and the absence of jadeite in this metagranite, a xenolith inclusion points to peak conditions of $P > 1.7$ GPa and $T = 600$–$650\,^{\circ}$C. These estimates are consistent with the peak conditions obtained from an associated mafic eclogite (2.0–2.2 GPa and 640–680 °C), as well as those reported from the previous literature on the Cellier Unit. This metagranite is of utmost interest to constrain the degree of transformation of quartzofeldspathic rocks during the HP event; it is similar and complementary to other key examples of poorly deformed metagranitoids from the Essarts and Malpica–Tuy units in the Variscan belt and the Monte Mucrone or Brossasco–Isasca units in the Alpine belt. Together with metahornfels of the same unit, La Picherais metagranite provides further evidence of continental subduction in the Ibero-Armorican Arc.

Data availability. The data that support the findings of this study are available in this article; further information is available from the corresponding author upon reasonable request.

Author contributions. TG: conceptualization; investigation; formal analysis; writing – original draft; visualization. PY: conceptualization; investigation; writing – review and editing; resources; funding acquisition. GG: conceptualization; investigation; formal analysis; writing – review and editing; resources.

Competing interests. The contact author has declared that none of the authors has any competing interests.

Disclaimer. Publisher's note: Copernicus Publications remains neutral with regard to jurisdictional claims in published maps and institutional affiliations.

Special issue statement. This article is part of the special issue "(Ultra)high-pressure metamorphism, from crystal to orogenic scale". It is a result of the 14th International Eclogite Conference (IEC-14) held in Paris and Lyon, France, 10–13 July 2022.

Acknowledgements. Philippe Yamato thanks the Institut Universitaire de France (2017–2022) for financial support. We thank Omar Boudouma, Michel Fialin and Nicolas Rividi for technical and analytical support. We thank the reviewers of this paper, Jacobi Abati and Simon Schorn, for their constructive comments, as well as Samuel Angiboust and Christian Chopin for their comments and editorial handling.

Financial support. This research has been supported by the IUF (grant 2017-2022, Philippe Yamato).

Review statement. This paper was edited by Samuel Angiboust and reviewed by Simon Schorn and Jacobo Abati.

References

Abati, J., Gerdes, A., Fernandez Suarez, J., Arenas, R., Whitehouse, M. J., and Diez Fernandez, R: Magmatism and early-Variscan continental subduction in the northern Gondwana margin recorded in zircons from the basal units of Galicia, NW Spain, GSA Bulletin, 122, 219–235, https://doi.org/10.1130/B26572.1, 2010.

Abers, G. A. and Hacker, B. R.: A MATLAB toolbox and Excel workbook for calculating the densities, seismic wave speeds, and major element composition of minerals and rocks at pressure and temperature, Geochem. Geophy. Geosy., 17, 616–624, https://doi.org/10.1002/2015GC006171, 2016.

Adjerid, Z., Godard, G., and Ouzegane, K.: High-pressure whiteschists from the Ti-N-Eggoleh area (Central Hoggar, Algeria): A record of Pan-African oceanic subduction, Lithos, 226, 201–216, https://doi.org/10.1016/j.lithos.2015.02.013, 2015.

Angiboust, S. and Harlov, D.: Ilmenite breakdown and rutile-titanite stability in metagranitoids: Natural observations and experimental results, Am. Mineral., 102, 1696–1708, https://doi.org/10.2138/am-2017-6064, 2017.

Austrheim, H.: Eclogitization of lower crustal granulites by fluid migration through shear zones, Earth Planet. Sc. Lett., 81, 221–232, https://doi.org/10.1016/0012-821X(87)90158-0, 1987.

Autran, A. and Peterlongo, J. M.: Massif Central, Revue des Sciences Naturelles d'Auvergne, 45, 5–123, 1973.

Baïsset, M., Labrousse, L., Yamato, P., and Schubnel, A.: Twinning and partial melting as early weakening processes in plagioclase at high pressure: insights from Holsnøy (Scandina-

vian Caledonides, Norway), Contrib. Mineral. Petrol., 178, 19, https://doi.org/10.1007/s00410-023-01998-x, 2023.

Baldwin, J., Powell, R., White, R., and Štípská, P.: Using calculated chemical potential relationships to account for replacement of kyanite by symplectite in high pressure granulites, J. Metamorph. Geol., 33, 311–330, https://doi.org/10.1111/jmg.12122, 2015.

Ballèvre, M. and Marchand, J.: Zonation du métamorphisme éclogitique dans la nappe de Champtoceaux (Massif armoricain, France), C. R. Acad. Sci. II, 312, 705–711, 1991.

Ballèvre, M., Marchand, J., Godard, G., Goujou, J.-C., Christian, J., and Wyns, R.: Eo-Hercynian events in the Armorican massif, in: Pre-Mesozoic geology in France and related areas, Springer, 183–194, https://doi.org/10.1007/978-3-642-84915-2_19, 1994.

Ballèvre, M., Capdevila, R., Guerrot, C., and Peucat, J.-J.: Discovery of an alkaline orthogneiss in the eclogite-bearing Cellier unit (Champtoceaux complex, Armorican massif): a new witness of the Ordovician rifting, C. R. Géosci., 334, 303–311, https://doi.org/10.1016/S1631-0713(02)01760-1, 2002.

Ballèvre, M., Bosse, V., Ducassou, C., and Pitra, P.: Palaeozoic history of the Armorican Massif: models for the tectonic evolution of the suture zones, C. R. Géosci., 341, 174–201, https://doi.org/10.1016/j.crte.2008.11.009, 2009.

Ballèvre, M., Martínez Catalán, J.R., López-Carmona, A., Pitra, P., Abati, J., Díez Fernández, R., Ducassou, C., Arenas, R., Bosse, V., Castiñeiras, P., Fernández-Suárez, J., Barreiro, J. G., Paquette, J.-L., Peucat, J.-J., Poujol, M., Ruffet, G., and Martínez, S. S.: Correlation of the nappe stack in the Ibero-Armorican arc across the Bay of Biscay: a joint French–Spanish project, in: The Variscan Orogeny: Extent, timescale and the formation of the European crust, Geol. Soc. Spec. Publ., 405, 77–113, https://doi.org/10.1144/SP405.13, 2014.

Bauville, A. and Yamato, P.: Pressure-to-depth conversion models for metamorphic rocks: derivation and applications, Geochem. Geophy. Geosy., 22, e2020GC009280, https://doi.org/10.1029/2020GC009280, 2021.

Bernard-Griffiths, J. and Cornichet, J.: Origin of eclogites from South Brittany, France: A Sm-Nd isotopic and REE study, Chem. Geol., 52, 185–201, https://doi.org/10.1016/0168-9622(85)90017-X, 1985.

Bidgood, A. K., Waters, D. J., Dyck, B. J., and Roberts, N. M.: The emplacement, alteration, subduction and metamorphism of metagranites from the Tso Morari Complex, Ladakh Himalaya, Mineral. Mag., 87, 40–59, https://doi.org/10.1180/mgm.2022.121, 2023.

Biino, G. G. and Compagnoni, R.: Very-high pressure metamorphism of the Brossasco coronite metagranite, southern Dora-Maira Massif, Western Alps, Schweiz. Mineral. Petrog. Mitt., 72, 347–363, 1992.

Bosse, V., Feraud, G., Ruffet, G., Ballèvre, M., Peucat, J.-J., and De Jong, K.: Late Devonian subduction and early-orogenic exhumation of eclogite-facies rocks from the Champtoceaux Complex (Variscan belt, France), Geol. J., 35, 297–325, https://doi/10.1002/gj.864, 2000.

Bras, E., Baïsset, M., Yamato, P., and Labrousse, L.: Transient weakening during the granulite to eclogite transformation within hydrous shear zones (Holsnøy, Norway), Tectonophysics, 819, 229026, https://doi.org/10.1016/j.tecto.2021.229026, 2021.

Brière, Y.: Les éclogites françaises, Leur composition minéralogique et chimique. Leur origine, Bulletin de la Société française de Minéralogie, 43, 72–222, https://doi.org/10.3406/bulmi.1920.3743, 1920.

Brun, J.-P. and Burg, J.-P.: Combined thrusting and wrenching in the Ibero-Armorican arc: a corner effect during continental collision, Earth Planet. Sc. Lett., 61, 319–332, https://doi.org/10.1016/0012-821X(82)90063-2, 1982.

Bruno, M. and Rubbo, M.: The metamorphic history of Monte Mucrone metagranodiorite constrained by garnet growth modelling, Period. Mineral., 75, 3–22, 2006.

Bruno, M., Compagnoni, R., and Rubbo, M.: The ultra-high pressure coronitic and pseudomorphous reactions in a metagranodiorite from the Brossasco-Isasca Unit, Dora-Maira Massif, western Italian Alps: a petrographic study and equilibrium thermodynamic modelling, J. Metamorph. Geol., 19, 33–43, https://doi.org/10.1046/j.1525-1314.2001.00291.x, 2001.

Catalán, J. M., Arenas, R., García, F. D., Cuadra, P. G., Gómez-Barreiro, J., Abati, J., Castiñeiras, P., Fernández-Suárez, J., Martínez, S. S., Andonaegui, P., Clavijo, E. G., Montes, A. D., Pascual, F. J. R., and Aguado, B. V.: Space and time in the tectonic evolution of the northwestern Iberian Massif: Implications for the Variscan belt, in: 4-D framework of continental crust, Vol. 200, Geological Society of America Memoir Boulder, Colorado, 403–423, https://doi.org/10.1130/2007.1200(21), 2007.

Cavet, P., Marchand, J., Gruet, M., Lardeux, H., Rivière, L. M., and Arnaud, A.: Carte géologique de la France (1 : 50 000), feuille Ancenis (452); notice explicative par Cavet, P., Arnaud, A., Blaise, J., Gruet, M., Lardeux, H., Marchand, J., Nicolas, A., Rivière, L. M., and Rossignol, J. C., 56 pp., BRGM, Orléans, 1987.

Chopin, C., Henry, C., and Michard, A.: Geology and petrology of the coesite-bearing terrain, Dora Maira massif, Western Alps, Eur. J. Mineral., 3, 263–291, https://doi.org/10.1127/ejm/3/2/0263, 1991.

Coggon, R. and Holland, T.: Mixing properties of phengitic micas and revised garnet phengite thermobarometers, J. Metamorph. Geol., 20, 683–696, https://doi.org/10.1046/j.1525-1314.2002.00395.x, 2002.

Cogné, J.: Une "nappe" cadomienne de style pennique: la série cristallophyllienne de Champtoceaux en bordure méridionale du Synclinal d'Ancenis (Bretagne-Anjou), Bulletin du Service de la carte géologique d'Alsace et de Lorraine, 19, 107–136, https://doi.org/10.3406/sgeol.1966.1300, 1966.

Compagnoni, R. and Maffeo, B.: Jadeite-bearing metagranites L.S. and related rocks in the Mount Mucrone area (Sesia-Lanzo zone, western Italian Alps), Schweizerische Miner. Petrog., 53, 355–378, 1973.

Connolly, J. A.: Multivariable phase diagrams; an algorithm based on generalized thermodynamics, Am. J. Sci., 290, 666–718, 1990.

Connolly, J. A.: Computation of phase equilibria by linear programming: a tool for geodynamic modeling and its application to subduction zone decarbonation, Earth Planet. Sc. Lett., 236, 524–541, https://doi.org/10.1016/j.epsl.2005.04.033, 2005.

Diener, J., Powell, R., White, R., and Holland, T.: A new thermodynamic model for clino-and orthoamphiboles in the system Na_2O–CaO–FeO–MgO–Al_2O_3–SiO_2–H_2O–O, J. Metamorph. Geol., 25, 631–656, https://doi.org/10.1111/j.1525-1314.2007.00720.x, 2007.

Doukkari, S. A., Diener, J. F., Ouzegane, K., and Kiénast, J.-R.: Mineral equilibrium modelling and calculated chemical potential relations of reaction textures in the ultrahigh temperature In Ouzzal terrane (In Hihaou area, Western Hoggar, Algeria), J. Metamorph. Geol., 36, 1175–1198, https://doi.org/10.1111/jmg.12441, 2018.

Dubuisson, F. R. A.: Catalogue de la collection minéralogique, géognostique et minéralurgique du département de la Loire-Inférieure, appartenant à la mairie de Nantes, Mellinet, Nantes, 319 pp., 1830.

Engvik, A. K., Austrheim, H., and Andersen, T. B.: Structural, mineralogical and petrophysical effects on deep crustal rocks of fluid-limited polymetamorphism, Western Gneiss Region, Norway, J. Geol. Soc., 157, 121–134, https://doi.org/10.1144/jgs.157.1.121, 2000.

Ferrando, S., Frezzotti, M., Petrelli, M., and Compagnoni, R.: Metasomatism of continental crust during subduction: the UHP whiteschists from the Southern Dora-Maira Massif (Italian Western Alps), J. Metamorph. Geol., 27, 739–756, https://doi.org/10.1111/j.1525-1314.2009.00837.x, 2009.

Gil Ibarguchi, J. I.: Petrology of jadeite metagranite and associated orthogneiss from the Malpica-Tuy allochthon (Northwest Spain), Eur. J. Mineral., 7, 403–416, https://doi.org/10.1127/ejm/7/2/0403, 1995.

Godard, G.: Petrology of some eclogites in the Hercynides: the eclogites from the southern Armorican massif, France, in: Eclogites and eclogites-facies rocks, Elsevier, 451–519, 1988.

Godard, G.: The Les Essarts eclogite-bearing metamorphic Complex (Vendée, Southern Armorican Massif, France), Géologie de la France, 2001, 19–51, 2001.

Godard, G.: Two orogenic cycles recorded in eclogite-facies gneiss from the southern Armorican Massif (France), Europ. J. Mineral., 21, 1173–1190, https://doi.org/10.1127/0935-1221/2009/0021-1984, 2009.

Godard, G., Kiénast, J.-R., and Lasnier, B.: Retrogressive development of glaucophane in some eclogites from "Massif Armoricain" (east of Nantes, France), Contrib. Mineral. Petrol., 78, 126–135, https://doi.org/10.1007/BF00373774, 1981.

Gosso, G., Messiga, B., Rebay, G., and Spalla, M. I.: Interplay between deformation and metamorphism during eclogitization of amphibolites in the Sesia–Lanzo Zone of the Western Alps, Int. Geol. Rev., 52, 1193–1219, https://doi.org/10.1080/00206810903529646, 2010.

Green, E., Holland, T., and Powell, R.: An order-disorder model for omphacitic pyroxenes in the system jadeite-diopside-hedenbergite-acmite, with applications to eclogitic rocks, Am. Mineral., 92, 1181–1189, 2007.

Guiraud, M., Powell, R., and Rebay, G.: H_2O in metamorphism and unexpected behaviour in the preservation of metamorphic mineral assemblages, J. Metamorph. Geol., 19, 445–454, https://doi.org/10.1046/j.0263-4929.2001.00320.x, 2001.

Hacker, B. R., Andersen, T. B., Johnston, S., Kylander-Clark, A. R., Peterman, E. M., Walsh, E. O., and Young, D.: High-temperature deformation during continental-margin subduction and exhumation: The ultrahigh-pressure Western Gneiss Region of Norway, Tectonophysics, 480, 149–171, https://doi.org/10.1016/j.tecto.2009.08.012, 2010.

Hawthorne, F. C., Oberti, R., Harlow, G. E., Maresch, W. V., Martin, R. F., Schumacher, J. C., and Welch, M. D.: Nomenclature of the amphibole supergroup, Am. Mineral., 97, 2031–2048, https://doi.org/10.2138/am.2012.4276, 2012.

Heinrich, C. A.: Kyanite-eclogite to amphibolite facies evolution of hydrous mafic and pelitic rocks, Adula nappe, Central Alps, Contrib. Mineral. Petrol., 81, 30–38, https://doi.org/10.1007/BF00371156, 1982.

Hobbs, B. E., Ord, A., Spalla, M. I., Gosso, G., and Zucali, M.: The interaction of deformation and metamorphic reactions, Geol. Soc., Lond. Spec. Publ., 332, 189–223, https://doi.org/10.1144/SP332.12, 2010.

Holland, T. and Powell, R.: An internally consistent thermodynamic data set for phases of petrological interest, J. Metamorph. Geol., 16, 309–343, https://doi.org/10.1111/j.1525-1314.1998.00140.x, 1998.

Holland, T. and Powell, R.: Activity–composition relations for phases in petrological calculations: an asymmetric multicomponent formulation, Contrib. Mineral. Petrol., 145, 492–501, https://doi.org/10.1007/s00410-003-0464-z, 2003.

Holland, T., Baker, J., and Powell, R.: Mixing properties and activity-composition relationships of chlorites in the system MgO-FeO-Al_2O_3-SiO_2-H_2O, Eur. J. Mineral., 10, 395–406, https://doi.org/10.1127/ejm/10/3/0395, 1998.

Holyoke, C. W. and Tullis, J.: The interaction between reaction and deformation: an experimental study using a biotite + plagioclase + quartz gneiss, J. Metamorph. Geol., 24, 743–762, https://doi.org/10.1111/j.1525-1314.2006.00666.x, 2006.

Kohn, M. J.: A refined zirconium-in-rutile thermometer, Am. Mineral., 105, 963–971, https://doi.org/10.2138/am-2020-7091, 2020.

Krabbendam, M., Wain, A., and Andersen, T. B.: Pre-Caledonian granulite and gabbro enclaves in the Western Gneiss Region, Norway: indications of incomplete transition at high pressure, Geol. Mag., 137, 235–255, 2000.

Kretz, R.: Symbols for rock-forming minerals, Am. Mineral., 68, 277–279, 1983.

Lacroix, A.: Etude pétrographique des éclogites de la Loire-Inférieure, Bulletin de la Société des Sciences naturelles de l'Ouest de la France, I, 81–114, 1891.

Lanari, P., Vidal, O., De Andrade, V., Dubacq, B., Lewin, E., Grosch, E. G., and Schwartz, S.: XMapTools: A MATLAB©-based program for electron microprobe X-ray image processing and geothermobarometry, Comput. Geosci., 62, 227–240, https://doi.org/10.1016/j.cageo.2013.08.010, 2014.

Lasnier, B., Leyreloup, A., and Marchand, J.: Découverte d'un granite charnockitique au sein de gneiss œillés; perspectives nouvelles sur l'origine de certaines leptynites du massif armoricain méridional (France), Contrib. Mineral. Petrol., 41, 131–144, https://doi.org/10.1007/BF00375038, 1973.

Le Bas, M. J., Maitre, R. L., Streckeisen, A., Zanettin, B., and IUGS Subcommission on the Systematics of Igneous Rocks: A chemical classification of volcanic rocks based on the total alkali-silica diagram, J. Petrol., 27, 745–750, https://doi.org/10.1093/petrology/27.3.745, 1986.

Li, D.-Y., Xiao, Y., Li, W.-Y., Zhu, X., Williams, H., and Li, Y.-L.: Iron isotopic systematics of UHP eclogites respond to oxidizing fluid during exhumation, J. Metamorph. Geol., 34, 987–997, https://doi.org/10.1111/jmg.12217, 2016.

Lotout, C.: Âge, durée et enregistrement du métamorphisme de haute pression dans le massif Central, Doctoral dissertation, Université Rennes 1, 2017.

Luisier, C., Baumgartner, L., Schmalholz, S. M., Siron, G., and Vennemann, T.: Metamorphic pressure variation in a coherent Alpine nappe challenges lithostatic pressure paradigm, Nat. Commun., 10, 1–11, https://doi.org/10.1186/s00015-021-00397-3, 2019.

Marchand, J., Sellier, D., Bossière, G., Carlier, G., Deniel, C., and Lasnier, B.: Carte géologique de la France (1/50000), feuille Savenay (450), 58 pp., BRGM, Orléans, 1989.

Martínez Catalán, J. R., Arenas, R., Díaz García, F., Rubio Pascual, F. J., Abati, J., and Marquínez, J.: Variscan exhumation of a subducted Paleozoic continental margin: the basal units of the Ordenes Complex, Galicia, NW Spain, Tectonics, 15, 106–121, https://doi.org/10.1029/95TC02617, 1996.

Matte, P.: Accretionary history and crustal evolution of the Variscan belt in Western Europe, Tectonophysics, 196, 309–337, https://doi.org/10.1016/0040-1951(91)90328-P, 1991.

Moulas, E., Burg, J. P., and Podladchikov, Y.: Stress field associated with elliptical inclusions in a deforming matrix: Mathematical model and implications for tectonic overpressure in the lithosphere, Tectonophysics, 631, 37–49, https://doi.org/10.1016/j.tecto.2014.05.004, 2014.

Palin, R. M., Reuber, G. S., White, R. W., Kaus, B. J., and Weller, O. M.: Subduction metamorphism in the Himalayan ultrahigh-pressure Tso Morari massif: an integrated geodynamic and petrological modelling approach, Earth Planet. Sc. Lett., 467, 108–119, https://doi.org/10.1016/j.epsl.2017.03.029, 2017.

Paquette, J.-L., Marchand, J., and Peucat, J.: Absence de tectonique cadomienne dans le complexe de Champtoceaux (Bretagne méridionale)? Comparaison des systèmes Rb-Sr et U-Pb d'un métagranite, Bull. Soc. Geol. France, 26, 907–912, https://doi.org/10.2113/gssgfbull.S7-XXVI.5.907, 1984.

Pearce, J. A.: Geochemical fingerprinting of oceanic basalts with applications to ophiolite classification and the search for Archean oceanic crust, Lithos, 100, 14–48, https://doi.org/10.1016/j.lithos.2007.06.016, 2008.

Peterman, E. M., Hacker, B. R., and Baxter, E. F.: Phase transformations of continental crust during subduction and exhumation: Western Gneiss Region, Norway, Eur. J. Mineral., 21, 1097–1118, https://doi.org/10.1127/0935-1221/2009/0021-1988, 2009.

Pitra, P., Ballèvre, M., and Ruffet, G.: Inverted metamorphic field gradient towards a Variscan suture zone (Champtoceaux Complex, Armorican Massif, France), J. Metamorph. Geol., 28, 183–208, https://doi.org/10.1111/j.1525-1314.2009.00862.x, 2010.

Pouchou, J.-L. and Pichoir, F.: Quantitative analysis of homogeneous or stratified microvolumes applying the model "PAP", in: Electron probe quantitation, Springer, 31–75, https://doi.org/10.1007/978-1-4899-2617-3_4, 1991.

Powell, R. and Holland, T.: Relating formulations of the thermodynamics of mineral solid solutions; activity modeling of pyroxenes, amphiboles, and micas, Am. Mineral., 84, 1–14, https://doi.org/10.2138/am-1999-1-201, 1999.

Proyer, A.: The preservation of high-pressure rocks during exhumation: metagranites and metapelites, Lithos, 70, 183–194, https://doi.org/10.1016/S0024-4937(03)00098-7, 2003.

Ribeiro, A., Pereira, E., Dias, R., Gil Ibarguchi, J., and Arenas, R.: Allochthonous sequences, in: Pre-Mesozoic Geology of Iberia, Springer, 220–246, https://doi.org/10.1007/978-3-642-83980-1_15, 1990.

Roda, M., Spalla, M. I., and Marotta, A. M.: Integration of natural data within a numerical model of ablative subduction: a possible interpretation for the Alpine dynamics of the Austroalpine crust, J. Metamorph. Geol., 30, 973–996, https://doi.org/10.1111/jmg.12000, 2012.

Rodríguez, J., Cosca, M., Gil Ibarguchi, J. I., and Dallmeyer, R.: Strain partitioning and preservation of $^{40}Ar/^{39}Ar$ ages during Variscan exhumation of a subducted crust (Malpica–Tui complex, NW Spain), Lithos, 70, 111–139, https://doi.org/10.1016/S0024-4937(03)00095-1, 2003.

Rubbo, M., Borghi, A., and Compagnoni, R.: Thermodynamic analysis of garnet growth zoning in eclogite facies granodiorite from M. Mucrone, Sesia Zone, Western Italian Alps, Contrib. Mineral. Petrol., 137, 289–303, https://doi.org/10.1007/s004100050551, 1999.

Rubie, D. C.: Role of kinetics in the formation and preservation of eclogites, Eclogite Facies Rocks, 111–140, 1990.

Rubie, D. C.: Disequilibrium during metamorphism: the role of nucleation kinetics, Geol. Soc. Lond. Spec. Publ., 138, 199–214, https://doi.org/10.1144/GSL.SP.1996.138.01.12, 1998.

Rumble, D.: Stable isotope geochemistry of ultrahigh-pressure rocks, in: When continents collide: Geodynamics and geochemistry of ultrahigh-pressure rocks, Springer, 241–259, https://doi.org/10.1007/978-94-015-9050-1_9, 1998.

Schorn, S.: Self-induced incipient "eclogitization" of metagranitoids at closed-system conditions, J. Metamorph. Geol., 40, 1271–1290, https://doi.org/10.1111/jmg.12665, 2022.

Schorn, S., Diener, J. F., Sorger, D., and Clark, C.: The contribution of charnockite magmatism to achieve near-ultrahigh temperatures in the Namaqua–Natal Metamorphic Province, South Africa, Lithos, 368, 105585, https://doi.org/10.1016/j.lithos.2020.105585, 2020.

Shand, S. J.: The Eruptive Rocks, 2nd edition, John Wiley, 444 pp., New York, 1943.

Spencer, K., Hacker, B., Kylander-Clark, A., Andersen, T., Cottle, J., Stearns, M., Poletti, J., and Seward, G.: Campaign-style titanite U–Pb dating by laser-ablation ICP: Implications for crustal flow, phase transformations and titanite closure, Chem. Geol., 341, 84–101, https://doi.org/10.1016/j.chemgeo.2012.11.012, 2013.

Streckeisen, A.: To each plutonic rock its proper name, Earth-Sci. Rev., 12, 1–33, https://doi.org/10.1016/0012-8252(76)90052-0, 1976.

Tropper, P., Essene, E. J., Sharp, Z. D., and Hunziker, J. C.: Application of K-feldspar–jadeite–quartz barometry to eclogite facies metagranites and metapelites in the Sesia Lanzo Zone (Western Alps, Italy), J. Metamorph. Geol., 17, 195–209, 1999.

Velde, B.: Les éclogites de la région nantaise (de Campbon au Cellier, Loire Atlantique), Bull. Mineral., 93, 370–385, https://doi.org/10.3406/bulmi.1970.6479, 1970.

Vernon, R. H.: Rapakivi granite problems: plagioclase mantles and ovoid megacrysts, Austr. J. Earth Sci., 63, 675–700, https://doi.org/10.1080/08120099.2016.1241953, 2016.

Vidal, P., Peucat, J., and Lasnier, B.: Dating of granulites involved in the Hercynian Fold-belt of Europe: an example taken from the granulite-facies orthogneisses at La Picherais, Southern Ar-

morican Massif, France, Contrib. Mineral. Petrol., 72, 283–289, https://doi.org/10.1007/BF00376146, 1980.

Vrabec, M., Janák, M., Froitzheim, N., and De Hoog, J. C.: Phase relations during peak metamorphism and decompression of the UHP kyanite eclogites, Pohorje Mountains (Eastern Alps, Slovenia), Lithos, 144, 40–55, https://doi.org/10.1016/j.lithos.2012.04.004, 2012.

Wain, A., Waters, D., and Austrheim, H.: Metastability of granulites and processes of eclogitisation in the UHP region of western Norway, J. Metamorph. Geol., 19, 609–625, https://doi.org/10.1046/j.0263-4929.2001.00333.x, 2001.

White, R. and Powell, R.: On the interpretation of retrograde reaction textures in granulite facies rocks, J. Metamorph. Geol., 29, 131–149, https://doi.org/10.1111/j.1525-1314.2010.00905.x, 2011.

Young, D. and Kylander-Clark, A.: Does continental crust transform during eclogite facies metamorphism?, J. Metamorph. Geol., 33, 331–357, https://doi.org/10.1111/jmg.12123, 2015.

Young, D. J., Hacker, B. R., Andersen, T. B., and Corfu, F.: Prograde amphibolite facies to ultrahigh-pressure transition along Nordfjord, western Norway: Implications for exhumation tectonics, Tectonics, 26, 15 pp., https://doi.org/10.1029/2004TC001781, 2007.

Zhao, Z.-F., Zheng, Y.-F., Gao, T.-S., Wu, Y.-B., Chen, B., Chen, F.-K., and Wu, F.-Y.: Isotopic constraints on age and duration of fluid-assisted high-pressure eclogite facies recrystallization during exhumation of deeply subducted continental crust in the Sulu orogen, J. Metamorph. Geol., 24, 687–702, https://doi.org/10.1111/j.1525-1314.2006.00662.x, 2006.